Biogeosciences, 23, 8617–8638, 2026
https://doi.org/10.5194/bg-23-8617-2026
© Author(s) 2026. This work is distributed under
the Creative Commons Attribution 4.0 License.

Biogeosciences Open Access EGU

Experimental evidence that organo-mineral interactions regulate dissolved organic matter composition and lability across permafrost landscapes of northwestern Canada

Gabrielle K. F. Hatten[1], Steven V. Kokelj[2], Sophie Opfergelt[3], Duane G. Froese[4], Alejandro Alvarez[4], Joseph M. Young[4], and Suzanne E. Tank[1]

[1]Department of Biological Sciences, University of Alberta, Edmonton, T6G 2G5, Canada
[2]Northwest Territories Geological Survey, Yellowknife, X1A 2L9, Canada
[3]Earth and Life Institute, Université catholique de Louvain, Louvain-la-Neuve, 1348, Belgium
[4]Department of Earth and Atmospheric Sciences, University of Alberta, Edmonton, T6G 2G5, Canada

Correspondence: Gabrielle K. F. Hatten (hatten@ualberta.ca)

Received: 1 April 2026 – Discussion started: 10 April 2026
Revised: 24 September 2026 – Accepted: 4 October 2026 – Published: 26 November 2026

Abstract. Increased land-water connectivity of northern landscapes driven by permafrost thaw is shifting the bioavailability of dissolved organic matter (DOM) in surface waters, with implications for northern food webs and regional and global carbon balances. However, sorption of DOM to previously frozen sediments has received little attention as a mechanism of regulating the bioavailability of organic matter in thaw-affected freshwater ecosystems. Using batch sorption experiments, we assessed sorption potential, water-extractable dissolved organic carbon (DOC) concentration, and the impact of sorption on DOM composition of six different permafrost sediment types common throughout northwestern Canada, reflecting variation in geologic and permafrost histories. A principal component analysis revealed that sediment biogeochemical characteristics reflected geologic origin, and past thaw increased within-type variation. Sorption was positively correlated with organo-reactive forms of Al and Fe and negatively correlated with sediment pH. Proportion of bulk sediment organic carbon released as water extractable DOC ranged from 1.0 % to 62.0 %, with yedoma sediments from the Klondike region releasing substantially more DOC than sediments from other regions. Preferential sorption of larger, humic-like compounds and displacement of mineral-bound small, aliphatic molecules enriched the DOM pool in labile compounds. Bio-incubations verified that exposure to sediments increased rates of biodegradation, corresponding with shifts in DOM composition and increased nutrient concentrations. Our experiments demonstrate that organo-mineral interactions have the potential to decrease DOC concentrations while increasing bioavailability of DOM remaining in solution, but that the strength of this response varies with sediment characteristics that are reflective of landscape history.

1 Introduction

As permafrost thaw increases across northern latitudes, biogeochemical constituents previously contained in permafrost become accessible for biological processing and lateral mobilization toward freshwater ecosystems and, ultimately, the coastal ocean (Vonk et al., 2019, 2025; Walvoord and Kurylyk, 2016). The lateral transport of permafrost carbon as dissolved organic carbon (DOC) is an important stimulant of change to the ecological and biogeochemical function of freshwater ecosystems. DOC is the microbially-accessible form of organic carbon in soils, freshwater, and the ocean, with organismal processing resulting in carbon mineralization into carbon dioxide and methane (Hanson et al., 2003; Lu et al., 2000; Yavitt, 1997). Molecular characteristics of dissolved organic matter (DOM), such as weight and molecular structure, impact DOM susceptibility to biodegradation (Arvola and Tulcnen, 1998; Catalán et al., 2021; Kalbitz et al., 2003). Across northern freshwater ecosystems, the im-

pact of permafrost thaw on DOC concentrations is regionally variable (Tank et al., 2020), with both substantial increases (e.g., Ewing et al., 2015; Mann et al., 2015) and decreases in DOC concentrations reported (e.g., Littlefair et al., 2017; Shakil et al., 2020). While permafrost thaw is generally associated with increases in DOM lability (e.g., Abbott et al., 2014; Littlefair and Tank, 2018; Mann et al., 2015; Vonk et al., 2013), permafrost-origin DOM shows wide compositional variation (MacDonald et al., 2021), and reduced lability has been observed in DOM originating from organic deposits (Burd et al., 2020; Wickland et al., 2018). Understanding controls on permafrost-origin organic matter concentration, composition, and lability both within and between regions is therefore critical for applications ranging from understanding local changes to ecological and food web function to upscaling the effects of thaw on the broader carbon cycle.

Within aquatic networks, the concentration of organic matter (OM) and its overall composition are in part regulated by interaction with minerals in soils, deposited sediments, and suspended particles in surface waters (e.g., Kaiser et al., 1996; Kalbitz et al., 2005; von Lützow et al., 2006). While these organo-mineral interactions are a well-established mechanism of OM stabilization in southern (i.e., non-permafrost) soils, these processes are only beginning to receive attention in the permafrost region. Organo-mineral interactions can provide physical (i.e., microbes cannot physically access OM) or physicochemical (i.e., increased activation energy required by microbes to access OM) protection of OM from biodegradation (von Lützow et al., 2006). Due to an increased number of potential bonding sites (Kaiser and Zech, 1997), large, aromatic molecules preferentially engage in organo-mineral interactions relative to small, aliphatic compounds (Hernes et al., 2007; Kothawala et al., 2014). The protection provided by organo-mineral interactions contributes to the persistence of OM in non-permafrost soils for centuries to millennia (Jastrow et al., 1996; Kleber et al., 2011; Rasmussen et al., 2005). Because permafrost thaw increases exposure of dissolved organics to mineral substrates via deepening flow pathways and lateral transport of sediments into river valleys, organo-mineral interactions may play an important role in regulating the ability of OM to occur in the dissolved state, and therefore its accessibility to microbes (Opfergelt et al., 2026).

Given that the potential for organo-mineral interactions is largely influenced by substrate properties (Kothawala et al., 2009; Rasmussen et al., 2018; Saidy et al., 2013), their influence on OM bioavailability likely varies across the permafrost domain. Variation in the genesis and evolution of landscapes has given rise to a diversity of contemporary permafrost landsystems with unique permafrost and substrate properties (Fig. 1) (Kokelj et al., 2026). Post-depositional transformations, such as mobilization or thaw and refreezing driven by geomorphic and paleoclimate factors, further increase diversity of permafrost landscapes by facilitating changes to sediment biogeochemistry and ground ice content at local to regional scales (Kokelj et al., 2026; Lacelle et al., 2004, 2019). Physical permafrost properties and terrain configuration influence local susceptibility to and mechanism of thaw under climate change (Grosse et al., 2011; Jorgenson et al., 2015; Kokelj et al., 2023, 2026), with biogeochemical implications for the interactions between surface waters and previously thawed sediments and the resulting impact on nearby aquatic ecosystems (Tank et al., 2020; Zolkos et al., 2022). For example, widespread increases in active layer thickness could facilitate the interaction between organic surface waters and previously frozen mineral-rich sediments (Keller et al., 2010; Mu et al., 2017; Speetjens et al., 2022), while permafrost mass-wasting occurring in ice-rich hillslopes transports terrestrial material into nearby aquatic ecosystems, enabling interaction between aquatic DOM and recently thawed mineral sediment (Kokelj et al., 2005; Littlefair et al., 2017; Shakil et al., 2022). This landscape variability in the nature of substrate and mechanism of thaw is becoming increasingly recognized as an important factor in understanding the impacts of climate-driven permafrost thaw on freshwater biogeochemistry and the fate of permafrost carbon (Opfergelt, 2020; Tank et al., 2020; Vonk et al., 2019).

To examine the potential for organo-mineral interactions between DOC and thawed permafrost sediments across varied landscapes, we sampled a broad range of sediment types from different permafrost landform assemblages with varying geological and permafrost histories across northwestern Canada. Sampling locations spanned several degrees of latitude and included subregions that experienced different landscape genesis and evolution processes (i.e., glaciated and unglaciated regions). We pursued three objectives: (a) to explore variation in sediment biogeochemical properties across different permafrost-affected sediment types found in northwestern Canada; (b) to experimentally determine the impact of organo-mineral interactions on DOC concentrations across these sediment types; and (c) to evaluate the impact of organo-mineral interactions on DOM composition and bioavailability. We hypothesized that mineral sediment that had experienced limited post-depositional transformation (i.e., syngenetic permafrost) would have the greatest potential for organo-mineral interactions due to its reduced exposure to past leaching and weathering processes. We expected exposure to thawed permafrost sediments to enrich the DOM pool in aliphatic compounds due to preferential sorption of aromatic compounds, and for this alteration to increase bioavailability of the remaining DOM pool. We use permafrost landsystems as a conceptual model (Kokelj et al., 2026) to better understand how the origin and evolution of permafrost landscapes controls on DOC concentrations and DOM composition in northern freshwater ecosystems and the variability of these potential interactions across the diverse Arctic region.

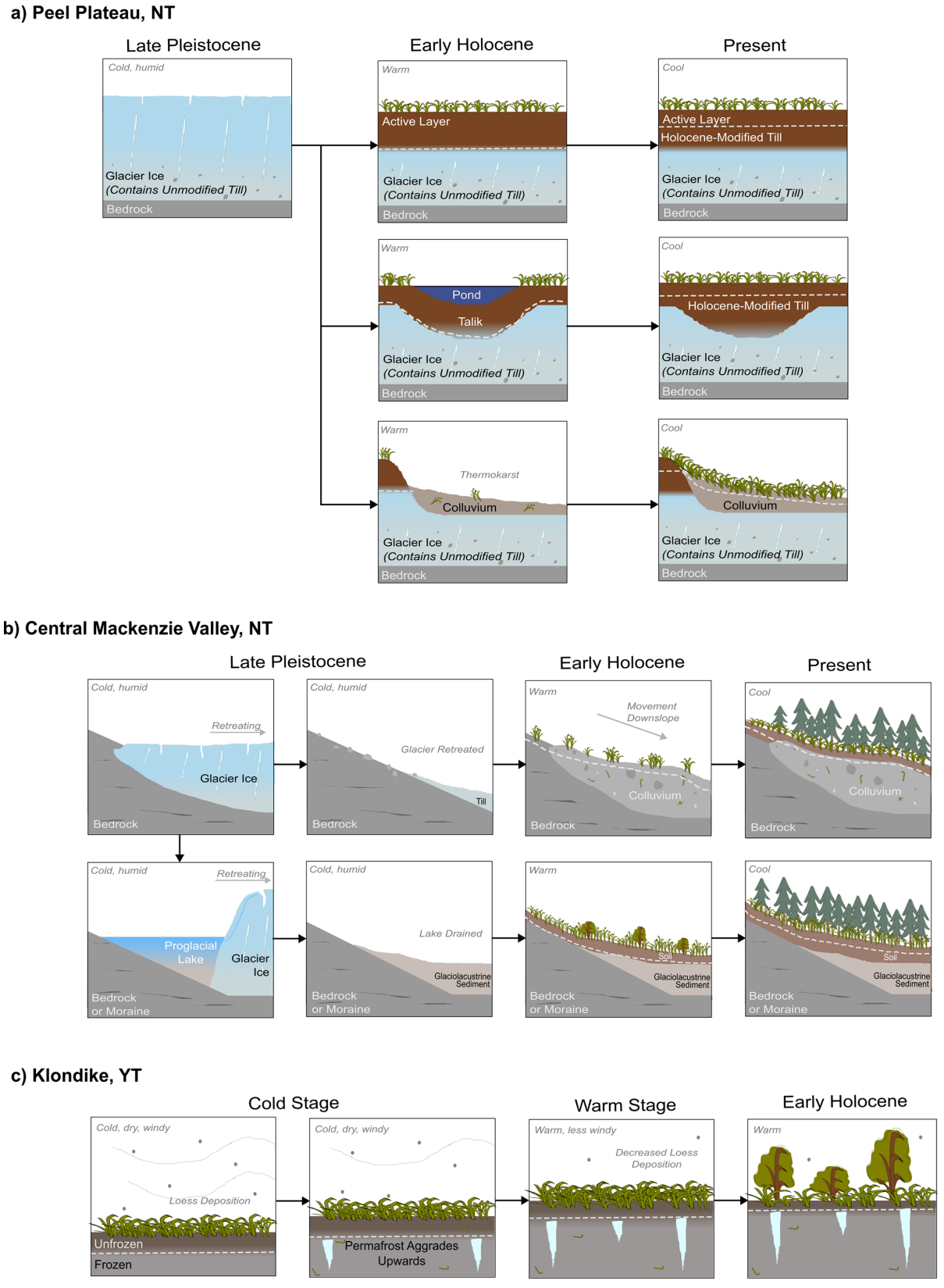

Figure 1. Emergence of distinct permafrost sediment types under different depositional environments, influenced by local topography and permafrost histories, in northwestern Canada. The permafrost table is denoted by a dashed line. Elements are not shown to scale. Note that additional sediment types exist in each region beyond those shown.

2 Methods

2.1 Study region

Northwestern Canada contains diverse landscapes shaped by glaciation, with climate-driven ecological and permafrost processes resulting in varied sediment biogeochemistry (Lacelle et al., 2019; MacDonald et al., 2021; Malone et al., 2013; Zolkos and Tank, 2020). The region is widely underlain by ice-rich permafrost, including segregated ice, wedge ice in tundra regions, and relict ice associated with permafrost-preserved moraine (Dyke and Evans, 2005; Lacelle et al., 2004, 2010; Mackay, 1972; O'Neill et al., 2019). Driven by warming temperatures, increasing summer precipitation, and legacy effects of wildfire, permafrost thaw-driven active layer thickening and mass-wasting features, such as retrogressive thaw slumps, are widespread throughout the region (Kokelj et al., 2017a, 2023; Lipovsky et al., 2005; O'Neill et al., 2023; Young et al., 2022). A diversity of permafrost landform assemblages characterizes the region, reflecting heterogeneity in geological and permafrost history, indicating substantial variation in physical and biogeochemical properties, mechanisms of thaw, and biophysical feedbacks. This provides an opportunity to assess the potential for organo-mineral interactions across a wide variety of sediment characteristics. In this study, samples were collected from three geologically distinct subregions.

The Peel Plateau (Gwich'in Settlement Area; Fig. 2b) is a fluvially incised, hummocky moraine landscape that extends from the Mackenzie Delta to the foothills of the Richardson Mountains in the Northwest Territories, Canada (Kokelj et al., 2017b). The region is within the Continuous Permafrost Zone (Heginbottom et al., 1995). The Peel Plateau was glaciated by the Laurentide Ice Sheet, which reached its maximum extent near the western margin of the Richardson Mountains in the late Pleistocene (18 000–15 000 years BP; Duk-Rodkin and Lemmen, 2000; Lacelle et al., 2013). This resulted in widespread emplacement of ice-rich moraine comprised of fine-grained material containing carbonates, silicates, pyrite, and gypsum derived from predominantly sedimentary shales and mudstones (Norris, 1980; Zolkos et al., 2018; Zolkos and Tank, 2020). Climate warming in the early Holocene (ca. 8000 years BP; Burn, 1997) caused thicker active layers, mass wasting, and talik development, thawing near-surface materials (Lacelle et al., 2004). Subsequent climate cooling and aggradation of permafrost have preserved this suite of modified materials, which are stratigraphically and biogeochemically distinct from the underlying debris-rich relict glacial ice and the overlying active layer (Malone et al., 2013). With present-day thaw, manifesting primarily as large retrogressive thaw slumps, sediments contained in relict glacial ice (hereafter referred to as *unmodified tills*) are exposed and eroded alongside more surficial *Holocene-modified tills* (i.e., contained in past taliks and paleo-active layers) and *colluvium* (i.e., modified tills with incorporated surface organics from past mass-wasting activity; Lacelle et al., 2019) (Fig. 1a). Thawed materials combine as *thawed debris* that is transported from the scar zone of these large mass-wasting features and deposited in debris tongues or valley-bottom streams (Kokelj et al., 2015, 2021). We collected samples from each of these permafrost "sediment types" that represent a continuum of permafrost materials ranging in depositional and thaw histories.

The central Mackenzie Valley (Sahtú Dene and Métis Settlement Area; Fig. 2c) is located east of the Mackenzie Mountains in the Northwest Territories, Canada in the Extensive Discontinuous Permafrost Zone and, at its high-altitude western limits, the Continuous Permafrost Zone (Brown et al., 1997; Heginbottom et al., 1995). Similar to the Peel Plateau, the region is characterized by fluvial incision, with exposed bedrock composed of North American margin sedimentary and metasediment origin rocks, including siliciclastic and carbonate units (Okulitch and Irwin, 2017). This region was overrun by the Laurentide Ice Sheet in the late Pleistocene (Dulfer et al., 2023; Kennedy et al., 2010), with the resulting surficial geology consisting of till with post-glacial lacustrine, alluvial, and colluvial deposits (Duk-Rodkin, 2018; Duk-Rodkin and Hughes, 2002). Thaw-driven landslides in the region expose ice-rich *glaciolacustrine* and till deposits and Holocene-aged *colluvium* deposits with incorporated local bedrock and surface organic materials (Fig. 1b) (Young et al., 2026, 2022). These permafrost sediment types, as well as *thawed debris*, were sampled from the central Mackenzie Valley.

The Klondike region (Tr'ondëk Hwëch'in Traditional Territory; Fig. 2d) in the central Yukon Territory contrasts the Peel Plateau and central Mackenzie Valley as it remained unglaciated during the Quaternary (Bostock, 1966; Froese et al., 2009). The Klondike region is located in the Discontinuous Permafrost Zone (Heginbottom et al., 1995). Pleistocene-aged permafrost in this region, referred to as yedoma, is primarily a result of loess deposition during Pleistocene cold stages, with aggradation of permafrost preserving accumulated sediments in a frozen state (Fig. 1c) (Froese et al., 2009; Schirrmeister et al., 2013, 2024). The organic carbon content and grain size of Klondike yedoma deposits vary with depth, reflecting hydroclimate-driven shifts in loess deposition and vegetation cover and productivity (Mahony, 2015; Sanborn et al., 2006). Bedrock in the Klondike region is predominantly composed of highly metamorphosed silicates (Mortensen, 1990). While biogeochemical properties (e.g., Ewing et al., 2015; Monhonval et al., 2021b; Strauss et al., 2012) and potential for organo-mineral interactions (Martens et al., 2023; Monhonval et al., 2021a) have been evaluated in yedoma from Eurasian and Alaskan permafrost environments, these properties have received little attention in Klondike yedoma (MacDonald et al., 2021). In the Klondike region, primary *yedoma* deposits (i.e., not mobilized since deposition) were sampled from exposures of sediment of different ages (site Mint Gulch (MG): ca. 13 200–16 140 years BP (Cocker et

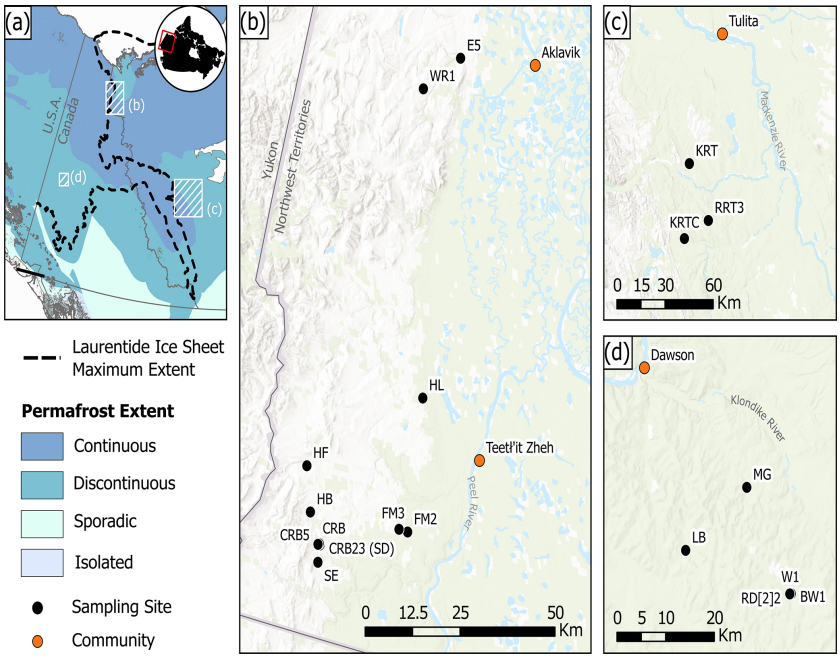

Figure 2. Sediment sampling locations in northwestern Canada. **(a)** Maximum extent of the Laurentide and Cordilleran ice sheets (dashed line) and permafrost extent in northwestern Canada, with three subregions indicated by white boxes with hash marks. Accompanying panels show sediment sampling locations (black) and nearby communities (red) within each subregion (**b** – Peel Plateau, NT; **c** – central Mackenzie Valley, NT; and **d** – Klondike region, YT). All sediment sampling locations fall within the glacial limit, except those in the Klondike region. Sampled sediment types and site codes are summarized in Table S1. *Sources*: Basemap – Designed and developed by Esri | Powered by Esri; Permafrost Extent – National Snow and Ice Data Centre (Brown et al., 2002); Glacial Limit – Dyke and Prest (1987); Provincial and Territorial Boundaries – Statistics Canada (2016). *Projection*: NAD83; Lambert Conformal Conic.

al., 2026); site Little Blanche (LB): associated with the Late Pleistocene Dawson tephra ca. 29 400 cal years BP (Demuro et al., 2008; Froese et al., 2002)) at multiple depths to capture climate-driven biogeochemical variation.

2.2 Sample collection and initial processing

To understand variation in biogeochemical properties and potential for organo-mineral interactions, sediment samples were collected from the above-described permafrost sediment types across the three study regions. A broad suite of samples was collected for biogeochemical characterization ($n = 76$), with a subset used for experimental determination of sorption potential ($n = 32$) and biodegradation ($n = 3$) (Table S1 in the Supplement). Permafrost samples were collected with a horizontal drill core from the headwalls of retrogressive thaw slumps (Peel Plateau and central Mackenzie Valley) or mining exposures (Klondike region). Thawed debris samples were collected from rills draining active retrogressive thaw slumps on the Peel Plateau and in the central Mackenzie Valley in the summer of 2023. Permafrost cores were kept frozen, and debris samples were immediately frozen after collection; samples were transported frozen to the Permafrost ArChives Science (PACS) laboratory at the University of Alberta, Canada and stored at −25 °C until processing.

Active layer samples were collected from each region to create stock solutions reflective of the DOM pool that may be encountered by permafrost sediments upon thaw. Active layer samples from the Peel Plateau were collected with a trowel from the exposed headwalls of four retrogressive thaw slumps (CRB, CRB5, HB, and HF; Fig. 2b and Table S1) with tussock- and shrub-tundra vegetation in July 2023. From the central Mackenzie Valley, an active layer sample was collected with a trowel within the undisturbed forested area adjacent to the retrogressive thaw slump KRT in June 2023. Active layer samples from the Klondike region were collected by vertical core in the summer of 2008 in the forested area in the Dominion Creek valley (sites W1, BW1, and RD[2]2 in Calmels et al., 2012, and Calmels and Froese, 2009). Active layer samples collected within each of the three regions were combined to create one representative sample for each region, as described below.

To remove materials that were thawed and potentially modified during the drilling process, the outer 0.5 cm of permafrost cores was removed using a rock saw with a diamond blade at −5 °C in the PACS laboratory cutting room. Cores were subsequently cut horizontally into 10 cm pucks. All samples were freeze-dried to remove water. Freeze-dried

samples were gently disaggregated and homogenized with a mortar and pestle and passed through a 2 mm mesh sieve (#10) before further processing (see below). Samples were further ground and sieved as required for each analysis. Prepared samples were stored in a dark freezer (−20 °C) until analysis.

2.3 Analysis of sediment biogeochemical properties

Grain size. Sieved samples (< 2 mm) were saturated with hydrogen peroxide (H_2O_2) to remove organics and dried overnight at 60 °C. Samples were treated with a solution of sodium hexametaphosphate ($Na_6[(PO_3)_6]$; 5 % w/w) and gently ground to prevent particle aggregation. Grain size, represented here as clay content (< 2 µm; %) and specific surface area ($m^2\,kg^{-1}$), was measured by laser diffraction analysis with a particle size analyzer (Mastersizer 3000; D422-ASTM, Malvern) in the PACS laboratory, with a lower detection limit of 10 nm. The mean of five measurements was recorded.

pH and conductivity. In a 50 mL centrifuge tube, 20 g of sediment (< 2 mm) was saturated with 40 mL (1 : 2 w/v) of 18.2 MΩ ultrapure (MilliQ) water and shaken at 60 rpm in the dark at room temperature for 2 h, following Pansu and Gautheyrou (2006). pH was measured with a calibrated benchtop pH probe (Mettler Toledo), and conductivity was measured with a calibrated YSI multiparameter probe (YSI Professional Plus). The mean of three measurements was recorded.

Carbon and nitrogen concentration. To assess percent sediment organic carbon (%SOC; mg OC per mg sediment) and nitrogen (%N), 15 mg of sediment (< 500 µm; #35 sieve) was weighed into silver (for SOC analysis) and tin (for N analysis) capsules. Capsules prepared for %SOC analysis were wetted with HCl (0.32 M trace metal grade) and heated to 60 °C in an enclosed container with 12 M HCl for 72 h to remove inorganic C (Harris et al., 2001; Ramnarine et al., 2011). Following fumigation, samples were neutralized with NaOH pellets in a desiccator for 24 h and dried at 60 °C for 16 h. Tungstic oxide (approximately 50 mg; WO_3) was added to each capsule to aid in combustion, and silver capsules were further encapsulated with tin. Samples for %N were analyzed without acidification. Elemental mass of C and N was measured by flash combustion with the Vario ISOTOPE Cube (Elementar) at the Ján Veizer Stable Isotope Laboratory at the University of Ottawa, Canada.

Mineral element concentrations. Total concentrations of mineral elements (Al_t, Ca_t, Fe_t, and Mn_t) were measured for all samples ($n = 79$) via nitric acid digestion. 25 mg of sediment (< 500 µm; #35 sieve) was treated with 10 mL of trace metal grade HNO_3 and digested for approximately 1 h using a microwave digestion system (MARS6; CEM Corp.). The digested sample was centrifuged and diluted before analysis. Selective extractions were performed on the subset of sediment samples selected for the batch sorption experiments ($n = 32$; see below) to target different phases of Al, Ca, Fe, and Mn. A dark ammonium oxalate extraction was performed to target poorly crystalline oxides and mineral elements complexed with organics (Blakemore et al., 1981; Monhonval et al., 2022). A sodium-pyrophosphate extraction was conducted to extract mineral elements complexed with organics and dispersible colloids (Bascomb, 1968; Parfitt and Childs, 1988). All extracted solutions were stored at 4 °C until analysis of Al, Fe, Mn, and Ca concentrations by Inductively Coupled Plasma Optical Emission spectroscopy (ICP-OES; Thermo Scientific ICAP6300) at the Biogeochemical Analytical Service Laboratory (BASL) at the University of Alberta. Element concentrations were normalized for the mass of sediment analyzed and expressed as mg of element per kg of sediment. Of the total pool, the reactive portion (i.e., highly reactive with organic compounds) of the Al, Fe, and Mn pools was assessed using the concentration extracted with ammonium oxalate (Al_o, Fe_o, and Mn_o; Monhonval et al., 2022). Because Ca oxalate precipitates, Ca concentrations from the ammonium oxalate extraction were not used (Monhonval et al., 2022). The portion of Al, Ca, Fe, and Mn in existing organo-metallic complexes is defined as the concentration extracted by sodium-pyrophosphate (Al_p, Ca_p, Fe_p, and Mn_p).

Mineralogy. Mineralogy of sediment samples (< 40 µm; #320 sieve) selected for batch sorption experiments ($n = 32$) were identified with X-ray diffraction (XRD) using front-loaded random powder mounts with an Ultima IV x-ray diffractometer (Rigaku, Tokyo, Japan) at the X-Ray Diffraction Laboratory in the Department of Earth and Atmospheric Sciences at the University of Alberta. Diffraction patterns were matched in the PDF 5+ database with the DIFFRAC.EVA v.6 software to produce presence-absence data, with a detection limit of 1 %–5 %.

Reference intensity ratios were used to determine relative mineral relative abundance (wt proportion) within sediments (Hubbard and Snyder, 1988), with an error range of 2 %–10 %.

Analytical methods and detection limits are summarized in Table S2.

2.4 Batch sorption experiments

Sorption properties of the selected subset of samples ($n = 32$) were determined through batch sorption experiments (e.g., Kaiser et al., 1996; Vance and David, 1989) that are designed to examine the proportion of DOC in solution that can be sorbed to minerals in specific sediment samples. Briefly, a consistent mass of sediment was added to individual replicates across a DOC dilution series created from active layer DOM extracts from the respective study regions, and carbon sorption potential was evaluated using the Initial Mass (IM) approach (Eq. 1; Nodvin et al., 1986) (Fig. S1). The IM approach relates the mass of carbon sorbed (RE) to the initial mass of carbon in each of the dilution series stocks

(X_i), with the y-intercept (b) representing the amount of carbon released from sediment in a carbon-free initial solution (i.e., water-extractable DOC; when $X_i = 0$) and the slope (m) representing a unitless sorption coefficient that describes the proportional increase in DOC sorbed per additional unit of DOC exposed to a fixed sediment mass. This relationship is expected to be linear until the sediment approaches its maximum sorption capacity. As all samples exhibited linear relationships in this study, the IM approach was selected over other methods of describing sorption relationships.

$$\mathrm{RE} = m \cdot X_i - b \quad (1)$$

To prepare for the batch sorption experiments, a regionally specific active layer leachate was extracted from the combined active layer material from each region by combining freeze-dried, gently ground sediment (< 2 mm) with MilliQ water (1 : 10 w/v) (Sect. S1 in the Supplement, Fig. S1). This mixture was agitated on a shaker table at 60 rpm for 72 h in the dark at 10 °C to restrict changes in DOM to sorption effects (i.e., limiting the influence of photodegradation or biological activity), before being filtered through a sterile polyethersulfone (PES) membrane filter (0.45 µm pore size; Sterlitech). The pH and conductivity of the organic leachates were adjusted to 6.5 (trace metal grade HCl) and 135 µS cm^{-1} (NaCl), respectively, to reflect natural stream conditions in the Peel Plateau (Kokelj et al., 2013; Malone et al., 2013; Zolkos et al., 2019). Leachates were diluted to create a 5-point dilution series, ranging from 0 % to 100 % of the initial leachate DOC concentration, using pH- and conductivity-adjusted MilliQ water. Batch sorption experiments were initiated by adding 5 g of sediment to 100 mL of each dilution (1 : 20 w/v) series, with each treatment conducted in duplicate (i.e., 10 experimental vials per incubation). After mixing for 48 h at 60 rpm in the dark at 10 °C, the solution was filtered through a sterile 0.45 µm PES filter. Aliquots for DOC concentration, DOM composition, pH, and conductivity were collected from the dilution series solutions prior to exposure, and from each of the 10 filtrates after exposure to sediment (Sect. S1). DOM composition was assessed with absorbance and fluorescence spectra, measured with an Aqualog UV 800 (HORIBA Scientific) optical spectrometer with a 10 mm quartz cuvette. Absorbance was measured from 240–800 nm at a 0.1 s integration time. Excitation-emission matrices (EEMs) were constructed using fluorescence measurements with excitation ranging 230–600 nm at 5 nm increments and emission ranging 118.78–828.18 nm at 2.33 nm increments. Integration time was adjusted between 1–3 s to achieve maximum values below 60 000 raw fluorescence units. Percent of soil OC vulnerable to extraction was determined as the molar ratio of water-extractable DOC to SOC (weDOC : SOC), measured as described above.

2.5 Bio-incubation experiments

To directly evaluate the impact of sorption-induced DOM compositional changes on DOM susceptibility to biodegradation, filtered solutions from select samples ($n = 3$) from the batch sorption experiment (unmodified till, Holocene-modified till, and thawed debris from Peel Plateau site SE) and a control bottle of MilliQ water were inoculated (10 % v/v inoculation) with water from the Mackenzie River (Gwich'in: *Nagwichoonji*; Inuvialuktun: *Kuuknak)*, collected 2 km upstream of Inuvik, NT (Sect. S2, Fig. S2). Stock solutions were evaluated for nutrients (total dissolved nitrogen [TDN], total dissolved phosphorous [TDP], ammonium [NH_4^+], nitrite / nitrate [NO_2^- / NO_3^-], and soluble reactive phosphorous [SRP]) prior to the start of the bio-incubation. Inoculated samples were incubated in triplicate for 14 days or until a 2 mg L^{-1} dissolved oxygen threshold was met to avoid anaerobic respiration. To evaluate biodegradation, dissolved carbon dioxide (measured as dissolved inorganic carbon following sample acidification; AS-C3 DIC Analyzer, Apollo SciTech, University of Alberta) was analyzed at the start and end of the experiment. Daily measurements of dissolved O_2 were additionally recorded using oxygen spot sensors (SP-PSt3-PSUP-YOPD5, PreSens GmbH) and a fibre-optic oxygen meter (Fibox 3; PreSens GmbH). Upon termination, changes in water chemistry were assessed via measurement of DOM composition, pH, and conductivity. Oxygen loss rate (k) was calculated as the exponential decay rate for the duration of the incubation.

2.6 Data treatment and analysis

Changes in DOM composition in the batch sorption and bio-incubation experiments were assessed using absorbance and fluorescence-based metrics. Spectral slope (275–295 nm; $S_{275–295}$) and slope ratio (275–295 nm slope: 350–400 nm slope; S_R), and specific ultraviolet absorbance at 254 nm ($SUVA_{254}$) were calculated from absorbance data as proxies for molecular weight and aromaticity of the DOM pool, respectively (Helms et al., 2008; Weishaar et al., 2003). A parallel factor (PARAFAC) analysis was conducted using EEMs with the drEEM toolbox (version 0.6.5) in MATLAB (The MathWorks Inc., 2023), following Murphy et al. (2013). To maximize robustness of the model, EEMs from both the batch sorption ($n = 374$) and bio-incubation ($n = 37$; $n_{total} = 411$) experiments were included in model construction. A 6-component model was validated, as discussed in Sect. 3.4. The relative contribution of each PARAFAC component to the overall fluorescence signal of a sample was determined by normalizing the maximum fluorescence scores of each component to the sum of all component intensities for the sample. Components were matched (similarity scores > 0.95 for both excitation and emission spectra) to published models on the OpenFluor database (Murphy et al., 2013) and compared to the traditional Coble peaks [B (tyrosine-like),

T (tryptophan-like), A (humic-like), M (marine or microbial humic-like), C (humic-like); Coble, 1996].

Statistical analyses were performed in R (4.4.1; R Core Team, 2024) unless otherwise noted, using *dplyr*, and *ggplot2* for data management and visualization (Wickham, 2016; Wickham et al., 2023). One-way analysis of variance (ANOVA), followed by Tukey's Honestly Significant Difference (HSD) test when main effects were significant ($p < 0.05$), were used to assess differences in biogeochemical properties. Paired t-tests were used to evaluate changes in pH and conductivity in the batch sorption experiment. The package *vegan* (Oksanen et al., 2024) was used to conduct principal component analyses (PCAs) for sediment biogeochemistry and DOM composition. Simple linear regressions (package *stats*) were used to relate sediment biogeochemical and sorption properties and to identify drivers of oxygen loss in the bio-incubation experiment. All summary statistics are reported as mean ± standard error, unless otherwise noted. See Sect. S3 in the Supplement for a detailed description of data analysis.

3 Results

3.1 Sediment mineralogy and biogeochemistry

Permafrost and debris sediments contained carbonates (dolomite, calcite, and siderite), pyrite, anatase, gypsum, and various silicate minerals (Table S3; Fig. S3). Quartz was the most abundant mineral detected in all samples (53.6 % ± 1.1). Albite and microcline were detected in all samples (11.1 % ± 1.0 and 5.7 % ± 0.3, respectively). Anatase and calcite were present in nearly all samples from the central Mackenzie Valley and Klondike region but were undetected in most samples from the Peel Plateau. Secondary clay minerals (i.e., kaolinite, illite, and/or montmorillonite) were present in all samples from the Peel Plateau and central Mackenzie Valley (12.3 % ± 0.7) but were not detected in yedoma samples. Non-silicate minerals were not detected in active layer samples.

Similar to mineralogy, biogeochemical properties of permafrost sediments varied between regions (Figs. S4, S5, and S6). Sediment pH ranged from 4.6 to 8.8, with most samples being slightly alkaline. Conductivity was significantly lower in sediment extracts from the central Mackenzie Valley ($224.4 \pm 17.0\,\mu S\,cm^{-1}$) compared to those from the Peel Plateau ($431.2 \pm 25.3\,\mu S\,cm^{-1}$, $p = 0.017$) and Klondike region ($527.1 \pm 79.3\,\mu S\,cm^{-1}$, $p = 0.022$). Clay content (%) was lowest in the Klondike samples (7.6 % ± 0.7), with similar clay content in sediments from the Peel Plateau (29.9 % ± 0.7) and central Mackenzie Valley (29.8 % ± 2.4). %SOC was highest in the Klondike samples (1.6 % ± 0.3), followed by the Peel Plateau (1.5 % ± 0.04) and central Mackenzie Valley samples (1.0 % ± 0.1). The ratio of SOC:N was highest in Peel Plateau samples (9.7 ± 0.2), followed by central Mackenzie Valley (8.1 ± 0.4) and Klondike samples (7.1 ± 0.4). Sediments from the Peel Plateau had significantly lower concentrations of total Ca_t ($4.4 \times 10^3 \pm 0.3 \times 10^3\,mg\,kg^{-1}$) and Mn_t ($2 \times 10^2 \pm 0.1 \times 10^2\,mg\,kg^{-1}$) compared to the central Mackenzie Valley ($1.5 \times 10^4 \pm 0.2 \times 10^4\,mg\,kg^{-1}$, $p < 0.001$; $4 \times 10^2 \pm 0.3 \times 10^2\,mg\,kg^{-1}$, $p < 0.001$) and Klondike ($1.5 \times 10^4 \pm 0.3 \times 10^4\,mg\,kg^{-1}$, $p < 0.001$; $4 \times 10^2 \pm 0.8 \times 10^2\,mg\,kg^{-1}$, $p < 0.001$). Sediments from the Peel Plateau had higher concentrations of reactive Al_o ($1.2 \times 10^3 \pm 0.1 \times 10^3\,mg\,kg^{-1}$) and Fe_o ($1.1 \times 10^4 \pm 0.1 \times 10^4\,mg\,kg^{-1}$) and lower complexed Ca_p ($2.1 \times 10^3 \pm 0.1 \times 10^3\,mg\,kg^{-1}$) compared to sediments from the central Mackenzie Valley and Klondike regions.

A PCA that considered concurrent variation in sediment biogeochemistry across all sites explained 51.5 % of sample variation across the first two principal component axes (Fig. 3). Principal component (PC) 1 (31.5 % of variation) described variation in mineral element (Al_t, Ca_t, Fe_t, and Mn_t) concentrations, with higher concentrations plotting positively along PC1. PC2 (25.0 % of variation) was associated with pH and OC content, with pH plotting positively and %SOC and the ratio of SOC:N plotting negatively along PC2. Within regions, sediment biogeochemistry varied by sediment type. In the Peel Plateau, unmodified tills showed substantial variation along PC1, reflecting differences in mineral element concentrations but little variation in pH or OC content between sites. Holocene-modified tills displayed greater variation in OC content and pH than unmodified tills, reflected in increased variation along PC2. Thawed debris displayed greater variation along both PC1 and PC2 than other sediment types. In the central Mackenzie Valley, samples clustered by site, reflecting different depositional origins (i.e., colluvium or glaciolacustrine) across sites. Yedoma samples also showed biogeochemical clustering by site. The %SOC was lower at site MG than at site LB, except for the youngest sample at MG (ca. 14 155 years BP; Cocker et al., 2026), which had considerably higher %SOC than the older samples at this site (14 485–16 140 years BP; Cocker et al., 2026). Samples from MG also had lower concentrations of mineral elements relative to samples from LB.

3.2 Sediment sorption properties

The prepared DOC dilution series varied between regions, ranging to $10\,mg\,L^{-1}$ for Peel Plateau samples, $52\,mg\,L^{-1}$ for central Mackenzie Valley samples, and $41\,mg\,L^{-1}$ for Klondike samples (Fig. S7). After exposure to sediment, both pH (7.4 ± 0.1; paired t-test: $t_{31} = 9.99$, $p < 0.001$) and conductivity ($272.8 \pm 20.6\,\mu S\,cm^{-1}$; paired t-test: $t_{31} = 7.89$, $p < 0.001$) were significantly higher than the initial solution (6.5 ± 0.01; $171.5 \pm 17.6\,\mu S\,cm^{-1}$). The relation between initial and sorbed bulk DOC was linear for all samples, indicating that no sample reached its maximum sorption capacity in the batch sorption experiments (Kaiser and

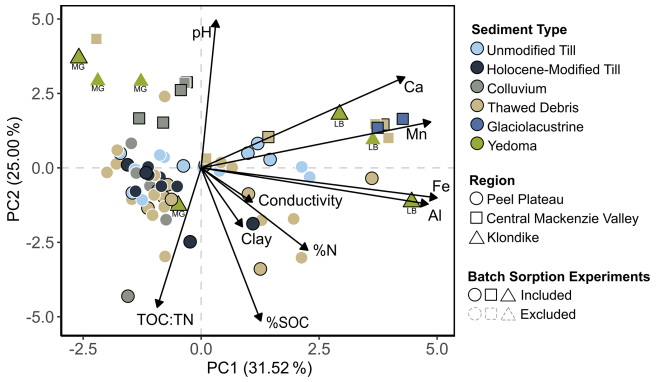

Figure 3. Principal component analysis (PCA) of sediment biogeochemical properties, with sediment type indicated by colour, and geographic region indicated by shape (Peel Plateau, NT ($n = 56$); central Mackenzie Valley, NT ($n = 13$); and Klondike region, YT ($n = 7$)). Data points outlined in black were evaluated for sorption properties with batch sorption experiments. Mineral element concentrations reflect total (Al, Ca, Fe, and Mn) fraction. Site labels are included for Klondike region samples (MG – Mint Gulch; LB – Little Blanche).

Zech, 1997). Sorption coefficients (m) ranged from −0.02 to 0.45, with higher coefficients occurring in sediments from the Peel Plateau (0.29 ± 0.02) compared to those from the central Mackenzie Valley (0.22 ± 0.02, $p < 0.160$) (Fig. 4; Table S4) and yedoma samples from the Klondike Region (0.17 ± 0.02, $p < 0.053$). The unmodified till sample from site CRB23 (PP_CRB23_UT) was the only sample with a sorption coefficient at or below 0 (−0.02). On the Peel Plateau, unmodified tills generally had lower sorption coefficients and thawed debris sediments had higher sorption coefficients than other sediment types at the same site (Fig. 4). In the central Mackenzie Valley, glaciolacustrine sediments generally had higher sorption coefficients than colluvium and thawed debris sediments.

Water-extractable DOC (b) ranged from 0.3 to 57.4 mg L^{-1} (Fig. 5; Table S4). When normalized for total OC content of the freeze-dried sediment samples (weDOC : SOC; i.e., the proportion of total SOC that was susceptible to water extraction), OC released ranged from 1.0 % to 62.0 %, with Klondike samples releasing substantially more OC (37.1 % ± 8.6), than samples from the Peel Plateau (5.2 % ± 0.6, $p < 0.001$) and central Mackenzie Valley (4.0 % ± 1.0, $p < 0.001$) (Fig. S8).

3.3 Relations between sediment characteristics and sorption properties

Across all regions, excluding the sample with a sorption coefficient near 0, m was positively correlated with the concentration of Al_o ($F_{1,29} = 4.50$, $p = 0.043$, $R = 0.36$) and Fe_o ($F_{1,29} = 4.45$, $p = 0.044$, $R = 0.36$), but negatively correlated with Ca_p ($F_{1,29} = 9.94$, $p = 0.004$, $R = 0.51$) and Mn_o ($F_{1,29} = 5.19$, $p = 0.030$, $R = 0.39$) (Fig. 6). These relationships, however, are not significant when considering only samples from within the Peel Plateau or central Mackenzie Valley regions (p ranged from 0.078–0.725). Sorption coefficients were negatively correlated with sediment pH ($F_{1,29} = 6.99$, $p = 0.013$, $R = 0.44$). There was no significant correlation between m and clay content ($F_{1,28} = 2.60$, $p = 0.118$, $R = 0.08$; Fig. S9a) or specific surface area ($F_{1,28} = 2.36$, $p = 0.136$, $R = 0.08$; Fig. S9b). Sediment OC (%SOC) was positively correlated with Al_p ($F_{1,29} = 12.99$, $p = 0.001$, $R = 0.56$) and Fe_p ($F_{1,29} = 39.01$, $p < 0.001$, $R = 0.75$) (Fig. S10). There was no significant relationship between %SOC and sorption coefficient ($F_{1,28} = 0.60$, $p = 0.444$, $R = 0.02$) (Fig. S11). The weDOC : SOC was positively correlated with Ca_p ($F_{1,29} = 20.58$, $p < 0.001$, $R = 0.65$) and clay content ($F_{1,29} = 29.71$, $p < 0.001$, $R = 0.71$) (relationships not shown). Across sediments containing secondary clay minerals (i.e., excluding yedoma samples), there was a positive correlation between illite relative abundance (wt proportion) and sorption coefficient ($F_{1,25} = 2.83$, $p = 0.107$, $R = 0.10$) and weDOC ($F_{1,25} = 5.62$, $p = 0.026$, $R = 0.18$) (Fig. S12b and d). However, there was no correlation between sorption coefficient ($F_{1,25} = 0.04$, $p = 0.851$, $R = 0.00$) or weDOC ($F_{1,25} = 0.77$, $p = 0.389$, $R = 0.03$) with kaolinite relative abundance (Fig. S12a and c). Montmorillonite was only detected in an active layer sample, which was not assessed for sorption properties.

3.4 Compositional shifts in DOM following sorption

A 6-component PARAFAC model was validated using split-half analysis, explaining 99.85 % of sample variance, with all components well-matched (similarity score > 0.95 for both excitation and emission spectra) within the OpenFluor database (Fig. S13; Table S5). The model consisted of two components (C1 and C2) representing aromatic, humic-like compounds of recent terrestrial origin. Components C3 and C4 were interpreted to reflect degraded humic-like compounds of terrestrial origin, while C5 was interpreted to reflect humic-like compounds of microbial origin. While the latter three components have similar EEM expressions, reflecting a "blue shift" from C1 and C2 along the emissions axis (Fig. S13), this shift can occur both through the diagenesis of terrigenous DOM (C3 and C4) and through the production of humic-like compounds by microbes (C5) (Coble, 1996; Coble et al., 1998). Our C5 was interpreted as microbially-produced humic material due to its close similarity to the M peak (marine or microbial humic), while C3 and C4 more closely aligned with the A and C peaks (humic-like) described by Coble (1996). The final component of the PARAFAC model (C6) reflected protein (tyrosine)-like compounds.

A PCA of optical indices (PARAFAC C1–6, $S_{275–295}$, S_R, and $SUVA_{254}$) was created for all samples ($n = 374$), with

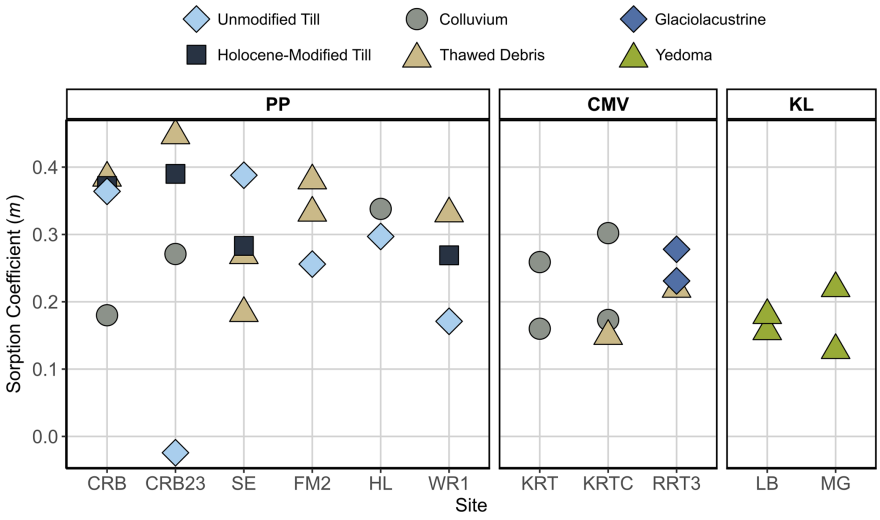

Figure 4. Sorption coefficients (m) of thawed permafrost sediments, demarcated by site (see Fig. 1 and Table S1) and geographic region (Peel Plateau, NT (PP); central Mackenzie Valley, NT (CMV); Klondike region, YT (KL)). Figure S7 shows the derivation of m for a subset of samples.

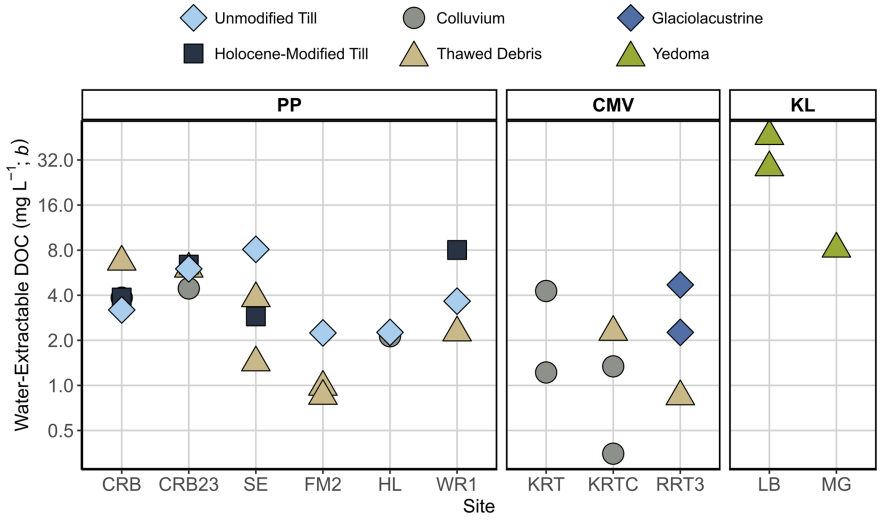

Figure 5. Water-extractable dissolved organic carbon (DOC; mg L^{-1}; b) of thawed permafrost sediments, demarcated by site (see Fig. 1 and Table S1) and geographic region (Peel Plateau, NT (PP); central Mackenzie Valley, NT (CMV); Klondike region, YT (KL)). Note that the y-axis is shown in log scale. Figure S7 shows the derivation of b for a subset of samples.

an explanatory power of 71.4 % across the first two principal component axes (Fig. S14a). Principal component 1 (PC1; 36.8 % of variation explained) is interpreted as a gradient of organic matter diagenesis, with PARAFAC C3 and C4 (degraded terrestrial material) plotting positively and C5 and C6 (microbially produced humic-like; protein-like) plotting negatively. Principal component 2 (PC2; 34.6 % of variation explained) describes variation in aromaticity and molecular weight, with $SUVA_{254}$, C1, and C2 (high aromaticity, humic-like) plotting negatively on this axis, and $S_{275–295}$ and S_R (lower molecular weight) plotting positively.

Water-extractable DOM (DOM composition at b) varied predominantly along PC2, driven by differences in molecular weight and aromaticity (Fig. S14b). Generally, water-extractable DOM from sediment samples from the central Mackenzie Valley was less aromatic and had lower molecular weight than samples from the other regions. Sediments from Klondike yedoma released DOM that appeared to be dominated by microbially produced DOM relative to other samples. Samples from the Peel Plateau showed the greatest variation across both PC1 and PC2, though this region also accounted for the greatest number of incubated samples.

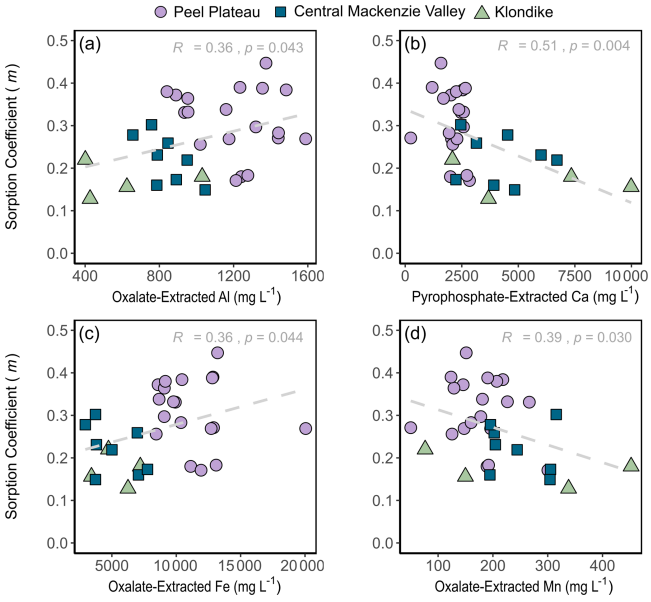

Figure 6. Relationships between sorption coefficient (m) and the reactive concentrations of elements (mg kg^{-1}) extracted by dark ammonium oxalate (**a** – Al_o, **c** – Fe_o, and **d** – Mn_o) or pyrophosphate (**b** – Ca_p). Simple linear regressions are represented by a dashed grey line with R and p values reported at the top of each panel.

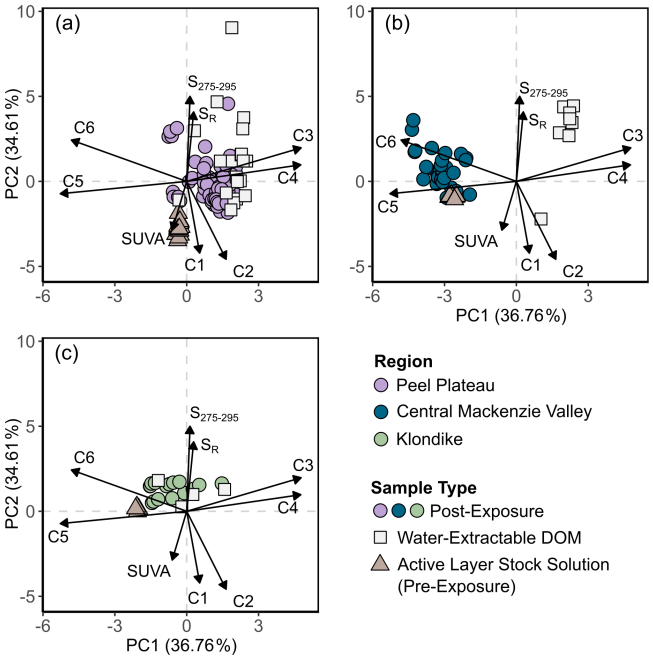

Figure 7. Shifts in dissolved organic matter (DOM) properties during batch sorption experiments. Principal component analysis (PCA) includes organic solutions pre- (triangle) and post-exposure to permafrost sediments (circle) and carbon-free water (squares; water-extractable DOM). Panels represent the same global PCA as Fig. S14a, with each panel displaying samples from three geographic regions: **(a)** Peel Plateau, NT; **(b)** central Mackenzie Valley, NT; and **(c)** Klondike region, YT.

After exposure to permafrost sediments, all organic solutions had a shift in DOM composition (Fig. 7), becoming enriched in aliphatic, low molecular weight compounds relative to the initial stock solution (positive shift along PC2). When exposed to permafrost sediments from the Peel Plateau and Klondike regions, the DOM pool contained more diagenetically altered terrestrial material (positive shift along PC1). In these samples, the DOM pool shifted to become more similar to the water-extractable DOM of the sediment. When exposed to sediments from the central Mackenzie Valley, the DOM pool became more saturated in microbially-derived compounds (negative shift along PC1).

Generally, samples showed greater sorption of C2 (terrestrial, humic-like) compounds than C6 (protein-like) compounds (Fig. S7). Displacement of labile compounds by humic-like compounds appeared to occur even in samples that demonstrated no bulk sorption of total DOC (e.g., unmodified till at site FM2; Fig. S7b). Despite having a linear slope for m when considering the total DOC pool, the sorption relationship appeared to reach an asymptote for C6 and C2 fluorescence in glaciolacustrine and debris sediments from RRT3 (Fig. S7c).

3.5 Changes to DOM susceptibility to biodegradation

To test DOM susceptibility to biodegradation following organo-mineral interactions, we inoculated active layer DOM extracts exposed to unmodified till, Holocene-modified till, and thawed debris from the Peel Plateau with a common microbial pool derived from water from the Mackenzie River. Sediment-exposed solutions were filtered prior to inoculation. As demonstrated in the batch sorption experiments, sediment-exposed DOM was enriched in aliphatic, low molecular weight compounds (positive shift along PC2) and contained more degraded terrestrial material (positive shift along PC1) relative to organic-rich leachates, with the most pronounced shift associated with the unmodified till sample (Fig. 8a). This shift was accompanied by increased NH_4 and TDN concentrations, with the greatest concentration associated with the unmodified till sample (1090 and 1640 µg L^{-1}, respectively) and lowest in the active layer control (20.9 and 411 µg L^{-1}, respectively). Across treatments, there was little variation in TDP (37–41 µg L^{-1}; range) and SRP (4–6 µg L^{-1}). Conductivity and pH ranged from 40.2–232.8 µS cm^{-1} and 6.8–7.4, respectively. DOC concentrations varied between 11.9–18.0 mg L^{-1}, with the highest concentration in the unmodified till treatment and the lowest concentration in the Holocene-modified till treatment. Biogeochemical parameters for each treatment at the start of the bio-incubation are summarized in Table S6.

The abiotic shift in DOM composition and increase in nitrogen corresponded to increased rates of DOC biodegradation. Dissolved oxygen depletion was most rapid in the un-

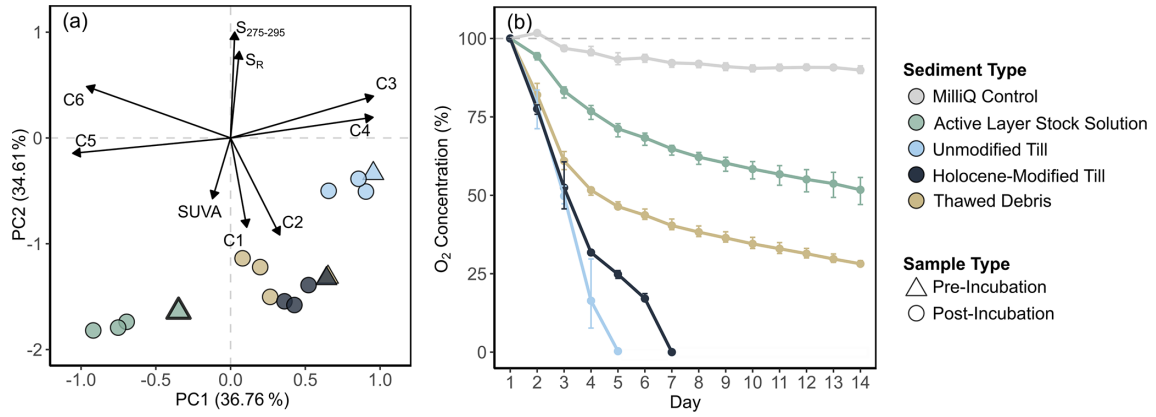

Figure 8. Change in dissolved organic matter (DOM) composition and dissolved oxygen (O_2) concentration over a 14 d incubation of sediment-exposed DOM with a microbial inoculum. **(a)** Principal component analysis (PCA) of DOM properties (same global PCA as Fig. S13a), showing solutions modified by organo-mineral interactions at the start and end of the bio-incubation. The green triangle with a bolded outline represents the initial active layer leachate, with other triangles reflecting change in DOM composition after exposure to thawed permafrost sediments. Circles represent the DOM composition at the end of the bio-incubation. **(b)** Consumption of dissolved oxygen throughout the bio-incubation, normalized to the initial oxygen concentration on Day 1. Error bars represent the range across 3 replicates.

modified till treatment ($k = -0.85 \pm 0.10$), in which all sample bottles became hypoxic by day 5 (Fig. 8b), followed by the Holocene-modified till treatment (-0.37 ± 0.01), in which all bottles became hypoxic on day 7. Sample bottles containing leachates that had not been exposed to sediments (active layer control) experienced the least oxygen depletion (-0.05 ± 0.003), but with oxygen depletion rates that were similar to the thawed debris treatment (-0.09 ± 0.003). No sample bottles with the thawed debris treatment or active layer control reached hypoxia throughout the 14 d bio-incubation.

Following bio-incubation, the DOM pool generally became enriched in protein-like and microbial-origin humic compounds (negative shift on PC1), but with slightly greater aromaticity and higher molecular weight (negative shift on PC2) (Fig. 8a). This shift in DOM composition was most pronounced in the active layer control sample bottles, and more modest for the till-associated treatments. Respiratory quotients (molar ratio between O_2 depletion and CO_2 production) ranged from 0.71–0.99 in sediment-exposed samples and 0.38–0.47 in the organic-rich leachate (Fig. S15).

Considering nutrient concentrations, DOC concentration, DOM composition (via PC1 and PC2 scores), pH, and conductivity prior to incubation, oxygen loss rate had a strong, positive association with NH_4 ($F_{1,2} = 467.40$, $p = 0.002$, $R = 0.99$) and TDN ($F_{1,2} = 333.30$, $p = 0.003$, $R = 0.99$). Positive associations between oxygen loss rate and DOM composition (treatment position on PC2; $F_{1,2} = 17.70$, $p = 0.052$, $R = 0.95$) and TDP ($F_{1,2} = 13.1$, $p = 0.069$, $R = 0.93$) were also observed (Fig. S16). Compared to these metrics, initial DOC concentration was a poor predictor of oxygen loss rate ($F_{1,2} = 3.40$, $p = 0.210$, $R = 0.79$) (Fig. S16).

4 Discussion

This research demonstrates that the bioavailability of the DOM pool is rapidly modified by organo-mineral interactions upon exposure to thawed permafrost sediments. Increased rates of OM biodegradation were associated with the enrichment of the DOM pool in labile compounds and higher nutrient concentrations, driven by the simultaneous release of labile compounds and sorption of humic-like compounds, and elevated concentrations of decomposition-origin NH_4^+ following exposure to sediments. The extent of the impact of organo-mineral interactions on DOC concentration and DOM composition varied by sediment type and by region, indicating that organo-mineral interactions facilitated by permafrost thaw and their impact on freshwater ecosystems will vary across the permafrost domain, but that this variation can be constrained based on knowledge of sediment geochemistry and landscape composition.

4.1 Organo-mineral interactions enrich DOM pool in labile compounds

Preferential sorption of humic-like, aromatic compounds was observed consistently across sample types in our batch sorption experiments (Fig. 7). Humic-like, high molecular weight, aromatic OM contains numerous functional groups available to participate in cation bridging and organo-metallic complexes (Kaiser and Zech, 1997), resulting in the preferential involvement of these compounds in organo-mineral interactions relative to low molecular weight, aliphatic molecules (Groeneveld et al., 2020; Hernes et al., 2007; Kothawala et al., 2014; Voggenreiter et al., 2024). Concurrently, the DOM pool can be enriched in labile compounds through the displacement of indigenous, low molecu-

lar weight, aliphatic OM by high molecular weight, aromatic compounds (Kaiser et al., 1996). The simultaneous occurrence of these processes is demonstrated in the unmodified till sample of site CRB23. While this sample had a bulk sorption coefficient near 0, changes to total C2 and C6 fluorescence values show a DOM exchange, whereby aromatic C2 was preferentially sorbed and protein-like C6 was preferentially released (Fig. S7) (Kaiser et al., 1996).

The simultaneous sorption of humic-like and release of aliphatic compounds at a relatively rapid timescale suggests that organo-mineral interactions have a "sorting effect" on DOM in impacted surface waters and hydrological flow paths (see also Shakil et al., 2022). The enrichment of permafrost-exposed waters in labile organic compounds and bioavailable nutrients corresponded with rapid biodegradation of OM in our bio-incubation experiments, resulting in a further shift of the DOM pool away from that which is released from permafrost (Fig. 8a). The sorting and protection of OM exposed to permafrost sediments may be a contributing mechanism to the relatively low lability of yedoma sediment OM (Kuhry et al., 2020), but high lability of DOM draining from yedoma deposits (Mann et al., 2015; Spencer et al., 2015; Vonk et al., 2013).

Variation in molecular weight and aromaticity of water-extractable DOM between sediment types (Fig. 7) aligns with past observations (Fouché et al., 2020; MacDonald et al., 2021, 2025). Differences in water-extractable DOM composition between unmodified and Holocene-modified tills likely reflect the progression of soil development and organic matter cycling during early Holocene thaw (Lacelle et al., 2019; MacDonald et al., 2021), whereby terrestrial-origin materials are decomposed and microbial-origin compounds are produced. Water-extractable DOM from yedoma tended to be enriched in protein-like and microbially-produced humic OM compared to other sediment types, aligning with previous observations of labile OM draining from yedoma in Siberia (Mann et al., 2015; Spencer et al., 2015) and Alaska (Drake et al., 2018; Ewing et al., 2015); likely the result of long-term biological activity under low oxygen environments found in syngenetic permafrost (Ewing et al., 2015), in combination with the sorting effects described above.

4.2 Landscape and permafrost history shape sediment biogeochemistry and organo-mineral interactions upon thaw

4.2.1 Biogeochemical properties

Past thaw history influenced the variability of biogeochemical properties in sediments in northwestern Canada (Fig. 3). On the Peel Plateau, the pronounced variability of thawed debris is likely reflective of the influence of inconsistent weathering and leaching processes experienced as sediments thaw and undergo transport (Monhonval et al., 2021a) and the integration of materials from multiple biogeochemically distinct sediment types. In contrast, unmodified tills, which have not been subjected to thaw-related modification, displayed the least within-type variation of sediments sampled on the Peel Plateau, even across different recessional fronts of the Laurentide Ice Sheet (MacDonald et al., 2025). Divergence of the characteristics of Holocene-modified tills from those of unmodified tills can be attributed to thaw-related processes, such as leaching of soluble minerals and past soil development. In the central Mackenzie Valley, geologic origin and thaw history resulted in biogeochemical divergence between sites. Permafrost sediments and thawed debris from sites with colluvium parent materials (KRT and KRTC; thawed in the early Holocene) had lower concentrations of mineral elements relative to sediments from features eroding glaciolacustrine deposits (RRT3), which had not thawed since post-depositional permafrost aggradation.

Biogeochemical variation in Klondike sediments may reflect differences in loess deposition and soil formation driven by hydroclimatic conditions. Samples from site LB (predating Dawson tephra; $> 29\,400$ years BP; Demuro et al., 2008; Froese et al., 2002) represent accumulation of materials driven by the deposition of carbonate-rich loess under cold stage conditions (colder temperatures, higher winds), resulting in high Ca concentrations (Monteath et al., 2023). A shift to warmer temperatures and weaker winds in the late Pleistocene (MG samples; ca. 13 500–15 900 years BP; Cocker et al., 2026) decreased loess deposition and stimulated the development of forests and associated soils, resulting in low mineral element concentrations and a shift in grain size (Péwé, 1975; Sanborn et al., 2006). Yedoma sediments at both sites generally had SOC content (%SOC; 0.57–2.66) at the lower range of previous observations in Pleistocene-aged yedoma from the Klondike (Fraser and Burn, 1997; MacDonald et al., 2021; Sanborn et al., 2006) and other regions (Schirrmeister et al., 2011; Strauss et al., 2013). At site MG, the youngest sample (ca. 13 500 years BP) had markedly higher OC content relative to deeper samples at that site, representing the transition from steppe-tundra to woody shrubland vegetation (Monteath et al., 2023; Murchie et al., 2021; Cocker et al., 2026). Concentrations of Al_t, Ca_t, Fe_t, and Mn_t of yedoma samples fell within the observed range for yedoma from Alaska and Siberia (Monhonval et al., 2021b), although at the lower end of each element's range, highlighting the distinct nature of Klondike yedoma relative to other regions of the Yedoma domain.

4.2.2 Sorption properties

Observed sorption coefficients (-0.02–0.45; Fig. 4) are lower than previously recorded for glacial-derived permafrost sediments in Siberia (0.43–0.60) (Kawahigashi et al., 2006) but align with the range observed in non-permafrost mineral soils (0.01–0.86; Kaiser et al., 1996, 2001; Kothawala et al., 2008). Compared to previous observations in the Peel Plateau (MacDonald et al., 2025; Zolkos

and Tank, 2019), unmodified tills released relatively high concentrations of water-extractable DOC (Fig. 5), despite similar assessment techniques. Several unmodified till samples used in this study were collected from different thaw exposures than previous studies, indicating variable weDOC within regional tills. Petrogenic DOC could have contributed to the high weDOC concentrations that we measured in unmodified tills (Bröder et al., 2021; Hilton et al., 2015), although the TN : TOC (total N : total OC) ratios of these sediments (0.095–0.128) are somewhat higher than other estimates for petrogenic sources that have been applied to the Mackenzie basin (0.064–0.078; Hilton et al., 2015). Yedoma samples released much higher proportions of their sediment OC than other sediment types, potentially influenced by high porewater DOC concentrations (Ewing et al., 2015) and associated low proportions of mineral-bound OC due to low sorption potentials of these sediments.

Thaw-related variation in biogeochemical properties translated to differences in sorption coefficients, aligning with observations of past thaw as a primary control on concentrations of mineral-associated OC in sediments on the Peel Plateau (Thomas et al., 2023). Across sediment types, sorption coefficients were likely influenced by the number of potential binding sites (influenced by mineral surface area and Al_t, Ca_t, Fe_t, and Mn_t concentrations) (e.g., von Lützow et al., 2006; Torn et al., 1997) and the presence of competitors (e.g., ions in solution measured by conductivity) for those binding sites (Gu et al., 1994; Guppy et al., 2005; Kaiser and Zech, 1997). Despite being a consistent predictor of sorption in non-permafrost soils (Abramoff et al., 2021; Burke et al., 1989; Hassink, 1997; Szymański et al., 2022), we did not observe a significant correlation between m and clay-sized particles or specific surface area, suggesting that competition for binding sites (e.g., by dissolved ions) may influence the potential for organo-mineral interactions in these sediments. The positive correlations observed between secondary clay minerals (i.e., relative abundances of kaolinite and illite) and both sorption coefficient and water-extractable DOC indicate that while these charged clays provide some stabilization of OC, these associations are reversible and may be susceptible to shifts in the biogeochemical setting (e.g., pH, dissolved ions) (Churchman et al., 2020; Saidy et al., 2013). As expected, Al_p and Fe_p were positively correlated with sorption across all sediment types (Fig. 6a and c). The absence of these relationships within regions, however, indicates that local lithology and past thaw history reduce the relative role of metal concentrations in OC stabilization in these landscapes. Likewise, the negative correlation observed between m and Ca_p when considering samples from all regions (Fig. 6b), contrasting with previous observations of Ca-mediated stabilization of OC, may be a reflection of region-specific lithology, particularly in samples from the Peel Plateau with low Ca paired with high sorption coefficients. Contrary to expectations, unmodified tills did not consistently have higher sorption coefficients than other sediment types at the same sites on the Peel Plateau.

We expected unmodified tills to have a high number of potential binding sites due to their high concentrations of reactive mineral elements (Al_o, Ca_p, Fe_o, Mn_o) and limited potential for previous organo-mineral interactions. However, competition for these binding sites from ions, as indicated by relatively high conductivity, may diminish the potential of these sediments to interact with organic compounds. High sorption coefficients observed in thawed debris sediments in the Peel Plateau could be explained by high concentrations of reactive Mn compared to other sediment types, as Mn can be an important OC binding agent even at low concentrations relative to Fe and Al. Low sorption coefficients observed in Klondike yedoma sediments likely arise from a combination of low potential binding sites, including the absence of secondary (charged) clays (e.g., kaolinite and illite), and high competition. High proportion of clay-sized particles and total mineral element concentrations relative to other sites (Fig. 3) would suggest that sediments at LB could have a high sorption potential, but this may be offset by high binding site competition (i.e., as assessed by high conductivity).

4.3 Implications for biological communities and biogeochemical cycling

Organo-mineral interactions have been proposed as a mechanism of protecting permafrost OC from biodegradation upon thaw (e.g., Wang et al., 2023), though this effect may be timescale-dependent. In our experiments, these interactions acted to rapidly sort the DOM pool, pulling humic-like compounds out of solution and releasing labile compounds, increasing overall lability of DOM in solution; combined with the release of bioavailable nitrogen, biodegradation of DOM was initially stimulated in filtered leachates exposed to permafrost sediments. DOM composition and nitrogen concentrations had a stronger influence on biodegradation rate than DOC concentration in our bio-incubation experiments (Fig. S16), indicating that a change in DOM composition and an increase in nutrient availability could supersede modest decreases in DOC concentrations in the short term, resulting in an immediate but short-lived increase in OM biodegradation. Similar to our observations, organo-mineral interactions increased DOC biodegradation in a river water sample from Sweden and were attributed to preferential sorption of aromatic compounds and resulting relative enrichment in more labile aliphatic molecules (Groeneveld et al., 2023). Despite this initial increase in biodegradation, the sorbed fraction of DOM is likely to experience long-term stabilization and remain relatively inaccessible to microbes (Jastrow et al., 1996; Kaiser and Guggenberger, 2000; Kleber et al., 2011; Rasmussen et al., 2005). The importance of this timescale factor is supported by a study with Siberian yedoma sediments that found increases in organo-mineral interactions corresponded to decreases in CO_2 and CH_4 emissions over a one-year pe-

riod (Jongejans et al., 2021; Monhonval et al., 2022). The influence of timescale on the relation between organo-mineral interactions and DOM will be important for understanding both immediate and long-term impacts of permafrost thaw on freshwater ecosystems.

Permafrost landform assemblages reflect variations in topography, substrate, and ground ice conditions, and hence, thaw trajectories (Kokelj et al., 2026), indicating that the susceptibility of DOM to organo-mineral interactions likely contrasts within and between regions with thaw (Opfergelt, 2020; Vonk et al., 2019). Increases in active layer thickness are widespread throughout the pan-Arctic, enabling percolation and flow of organic surface waters into deeper, mineral-rich sediments (Keller et al., 2010; Mu et al., 2017), facilitating opportunities for the creation and mobilization of mineral-bound OC (Herndon et al., 2017; Hirst et al., 2022). On the Peel Plateau, this is evidenced by increased concentrations of organic carbon complexed with metals in near surface, previously thawed and refrozen tills relative to unmodified tills, indicating that increases in active layer thickness facilitated organo-mineral interactions in this region during the early Holocene (Thomas et al., 2023). In contrast to increases in active layer thickness, mass-wasting events are more localized but cause dramatic increases in the transport of sediment and associated biogeochemical constituents within impacted fluvial networks (Keskitalo et al., 2021; Malone et al., 2013; Zolkos et al., 2020). Organo-mineral interactions facilitated by the direct mixing of thawed permafrost materials and their intersection with surface water DOM may result in more pronounced, but localized impacts on DOC concentrations and DOM bioavailability (e.g., Littlefair et al., 2017; Shakil et al., 2022). The mechanism of contemporary permafrost thaw, shaped by landscape history (Kokelj et al., 2026), directly influences how sediment is delivered to and interacts with surface waters, wielding strong control on the facilitation of organo-mineral interactions.

In addition to the influence of thaw mechanism, the impacts of organo-mineral interactions on carbon sequestration and OM bioavailability will be affected by substrate characteristics across different permafrost landsystems (sensu Kokelj et al., 2026; Tank et al., 2020). Variation in composition and bioavailability of permafrost-origin DOM has previously been observed across permafrost sediment types on the Peel Plateau (Lacelle et al., 2019; MacDonald et al., 2021, 2025). Notably, our study primarily included sediments exposed by retrogressive thaw slumps, comprising environments with ice-rich fine-grained mineral soils, necessarily excluding lowland, organic-rich landforms such as permafrost peatlands or drained lake basins that have co-developed with permafrost under different climate, geomorphologic and ecosystem conditions (Kokelj et al., 2026; Wolfe et al., 2020; Zoltai, 1993). However, we demonstrate a high degree of variability within sediment types, particularly in those that have undergone past thaw, highlighting important considerations for upscaling and support for using a landsystem approach that considers geological legacy and permafrost history as drivers of variation in sediment properties (Kokelj et al., 2026). Biogeochemical conditions within recipient freshwater ecosystems will also impact the stability of organo-mineral interactions; for example, via cleavage of existing organo-mineral bonds under anoxic conditions, and subsequent release of DOM and redox-sensitive metals (Lau et al., 2024; Peter et al., 2016). Given their role in protecting OM from biodegradation over centuries to millennia (Jastrow et al., 1996; Kleber et al., 2011; Rasmussen et al., 2005), the potential for organo-mineral interactions should be explored broadly, under different biogeochemical conditions reflective of the variation in sediment properties and manifestation of thaw across permafrost environments.

5 Conclusions

Through controlled batch sorption and bio-incubation experiments, we addressed three key objectives, examining organo-mineral interactions between DOM and thawed permafrost sediments from northwestern Canada. First, we documented substantial variation in sediment biogeochemical properties, both within and across permafrost sediment types, linked to geologic origin and thaw history. Second, we experimentally demonstrated interactions between DOM and permafrost-origin sediments, resulting in shifts in DOM composition and DOC concentrations. Third, we confirmed that exposure to thawed permafrost sediments increased biodegradation rates, driven by shifts in DOM composition and nutrient concentrations. Contrary to our hypotheses, syngenetic yedoma sediments did not exhibit the highest sorption potential; instead, these sediments released substantial DOC and demonstrated limited sorption compared to glaciogenic sediment types. However, our hypotheses regarding enrichment of the DOM pool in bioavailable compounds were supported by our batch sorption and bio-incubation experiments. The simultaneous sorption of high molecular weight, aromatic compounds and release of low molecular weight, aliphatic compounds, combined with the release of bioavailable nutrients from sediments, resulted in increased biodegradation rates.

Our experiments demonstrate that exposure to thawed permafrost sediments has the potential to increase biodegradation rates of DOM in the short-term, contributing to our understanding of aquatic biogeochemical and biological responses to thaw. The influence of organo-mineral interactions on DOC concentrations and DOM composition varied within and across geographic regions, with past thaw increasing within-type variation, indicating the importance of incorporating geologic origin and past thaw history in understanding the composition of permafrost and thaw-driven impacts on northern aquatic ecosystems. Further, our experiments demonstrate the protection of a portion of permafrost-origin carbon from biodegradation, supporting the consider-

ation of stabilization via organo-mineral interactions as a potential pathway for permafrost carbon upon thaw in carbon cycle models.

Data availability. Sediment characteristics and water chemistry data from experiments are available on the Borealis Dataverse repository (https://doi.org/10.5683/SP3/NFOPAF, Hatten et al., 2026).

Supplement. The supplement related to this article is available online at https://doi.org/10.5194/bg-23-8617-2026-supplement.

Author contributions. GKFH and SET designed the study, with contributions from all authors. Field samples were collected by GKFH, SET, SVK, AA, JMY, and DGF. GKFH led data analysis and manuscript writing, with contributions from all authors. Funding was procured by all authors.

Competing interests. The contact author has declared that none of the authors has any competing interests.

Disclaimer. Publisher's note: Copernicus Publications remains neutral with regard to jurisdictional claims made in the text, published maps, institutional affiliations, or any other geographical representation in this paper. The authors bear the ultimate responsibility for providing appropriate place names. Views expressed in the text are those of the authors and do not necessarily reflect the views of the publisher.

Acknowledgements. This work took place in the Gwich'in Settlement Area, Sahtú Dene and Métis Settlement Area, and Tr'ondëk Hwëch'in Traditional Territory. We are grateful for the contributions and hospitality of the communities of Inuvik, Fort McPherson (Tetlit Zheh), Norman Wells, and Tulit'a. We thank the Aurora Research Institute the Gwich'in Renewable Resources Board, the Gwich'in Tribal Council, and the Sahtu Renewable Resources Board for their support. We thank A. Koe, J. Yakeleya, W. Charlie, M. Taskovic, and M. Pusch for assistance in the field. This work was conducted under Northwest Territories research licence #5597 (SET). We thank the Northwest Territories Geological Survey for their support (NTGS Contribution #0179).

Financial support. This research has been supported by Polar Knowledge Canada (grant no. 621-23 (SET)), the Northern Scientific Training Program (GKFH), the University of Alberta Northern Research Awards (GKFH), the Natural Sciences and Engineering Research Council of Canada (grant nos. 2019-05524 (SET), 2019-444873 (SET), RGPIN-2019-06820 (DGF), 305449-2019 (DGF), and 575207 (SET and DF); Canada Graduate Scholarship – Master's (GKFH)), and the Fund for Scientific Research (FNRS) in Belgium (grant no. FC69480 (SO)).

Review statement. This paper was edited by David Janssen and reviewed by two anonymous referees.

References

Abbott, B. W., Larouche, J. R., Jones, J. B., Bowden, W. B., and Balser, A. W.: Elevated dissolved organic carbon biodegradability from thawing and collapsing permafrost, J. Geophys. Res.-Biogeo., 119, 2049–2063, https://doi.org/10.1002/2014JG002678, 2014.

Abramoff, R. Z., Georgiou, K., Guenet, B., Torn, M. S., Huang, Y., Zhang, H., Feng, W., Jagadamma, S., Kaiser, K., Kothawala, D., Mayes, M. A., and Ciais, P.: How much carbon can be added to soil by sorption?, Biogeochemistry, 152, 127–142, https://doi.org/10.1007/s10533-021-00759-x, 2021.

Arvola, L. and Tulcnen, T.: Effects of allochthonous dissolved organic matter and inorganic nutrients on the growth of bacteria and algae from a highly humic lake, Environ. Int., 24, 509–520, https://doi.org/10.1016/S0160-4120(98)00045-2, 1998.

Bascomb, C. L.: Distribution of pyrophosphate-extractable iron and organic carbon in soils of various groups, J. Soil. Sci., 19, 251–268, https://doi.org/10.1111/j.1365-2389.1968.tb01538.x, 1968.

Blakemore, L. C., Searle, P. L., and Daly, B. K.: Methods for chemical analysis of soils, Department of Scientific and Industrial Research, 102 pp., https://doi.org/10.7931/DL1-SBSR-10A, 1981.

Bostock, H. S.: Notes on glaciation in central Yukon Territory, Geological Survey of Canada, 65–36, https://doi.org/10.4095/100937, 1966.

Bröder, L., Keskitalo, K., Zolkos, S., Shakil, S., Tank, S. E., Kokelj, S. V., Tesi, T., Van Dongen, B. E., Haghipour, N., Eglinton, T. I., and Vonk, J. E.: Preferential export of permafrost-derived organic matter as retrogressive thaw slumping intensifies, Environ. Res. Lett., 16, 054059, https://doi.org/10.1088/1748-9326/abee4b, 2021.

Brown, J., Ferrians, O., Heginbottom, J. A., and Melnikov, E. S.: Circum-Arctic map of permafrost and ground-ice conditions, Circum-Pacific Map, 45, U.S. Geological Survey, https://doi.org/10.3133/cp45, 1997.

Brown, J., Ferrians, O., Heginbottom, J. A., and Melnikov, E.: Circum-Arctic map of permafrost and ground-ice conditions (GGD318, Version 2), Boulder, Colorado USA. National Snow and Ice Data Center [data set], https://doi.org/10.7265/skbg-kf16, 2002.

Burd, K., Estop-Aragonés, C., Tank, S. E., and Olefeldt, D.: Lability of dissolved organic carbon from boreal peatlands: interactions between permafrost thaw, wildfire, and season, Can. J. Soil. Sci., 100, 503–515, https://doi.org/10.1139/cjss-2019-0154, 2020.

Burke, I. C., Yonker, C. M., Parton, W. J., Cole, C. V., Flach, K., and Schimel, D. S.: Texture, climate, and cultivation effects on soil organic matter content in U.S. grassland soils, Soil Sci. Soc. Am. J., 53, 800–805, https://doi.org/10.2136/sssaj1989.03615995005300030029x, 1989.

Burn, C. R.: Cryostratigraphy, paleogeography, and climate change during the early Holocene warm interval, western Arctic coast, Canada, Can. J. Earth Sci., 34, 912–925, https://doi.org/10.1139/e17-076, 1997.

Calmels, F. and Froese, D. G.: Cryostratigraphic record of permafrost degradation and recovery following historic surface disturbances, Klondike area, Yukon, Yukon Exploration and Geology 2008, Yukon Geological Survey, https://emrlibrary.gov.yk.ca/ygs/yeg/2008/2008_p085-098.pdf (last access: 10 November 2024), 2009.

Calmels, F., Froese, D. G., and Clavano, W. R.: Cryostratigraphic record of permafrost degradation and recovery following historic (1898–1992) surface disturbances in the Klondike region, central Yukon Territory, Can. J. Earth Sci., 49, 938–952, https://doi.org/10.1139/e2012-023, 2012.

Catalán, N., Pastor, A., Borrego, C. M., Casas-Ruiz, J. P., Hawkes, J. A., Gutiérrez, C., Von Schiller, D., and Marcé, R.: The relevance of environment vs. composition on dissolved organic matter degradation in freshwaters, Limnol. Oceanogr., 66, 306–320, https://doi.org/10.1002/lno.11606, 2021.

Churchman, G. J., Singh, M., Schapel, A., Sarkar, B., and Bolan, N.: Clay minerals as the key to the sequestration of carbon in soils, Clay. Clay Miner., 68, 135–143, https://doi.org/10.1007/s42860-020-00071-z, 2020.

Coble, P. G.: Characterization of marine and terrestrial DOM in seawater using excitation-emission matrix spectroscopy, Mar. Chem., 51, 325–346, https://doi.org/10.1016/0304-4203(95)00062-3, 1996.

Coble, P. G., Del Castillo, C. E., and Avril, B.: Distribution and optical properties of CDOM in the Arabian Sea during the 1995 Southwest Monsoon, Deep-Sea Res. Pt. II, 45, 2195–2223, https://doi.org/10.1016/S0967-0645(98)00068-X, 1998.

Cocker, S. L., Francis, E., Wanket, C., Monteath, A. J., Kuzmina, S., Tirlea, D., Jensen, B. J. L., Heintzman, P. D., Shapiro, B., and Froese, D. G.: Latest Pleistocene shrub expansion and steppe-tundra persistence in easternmost Beringia, Quaternary Sci. Rev., 388, 110081, https://doi.org/10.1016/j.quascirev.2026.110081, 2026.

Demuro, M., Roberts, R. G., Froese, D. G., Arnold, L. J., Brock, F., and Ramsey, C. B.: Optically stimulated luminescence dating of single and multiple grains of quartz from perennially frozen loess in western Yukon Territory, Canada: Comparison with radiocarbon chronologies for the late Pleistocene Dawson tephra, Quat. Geochronol., 3, 346–364, https://doi.org/10.1016/j.quageo.2007.12.003, 2008.

Drake, T. W., Raymond, P. A., and Spencer, R. G. M.: Terrestrial carbon inputs to inland waters: A current synthesis of estimates and uncertainty, Limnol. Oceanogr. Lett., 3, 132–142, https://doi.org/10.1002/lol2.10055, 2018.

Duk-Rodkin, A.: Surficial geology, Dahadinni River, Northwest Territories, NTS 95-N northwest, Canadian Geoscience Map 298, Geological Survey of Canada, https://doi.org/10.4095/299113, 2018.

Duk-Rodkin, A. and Hughes, O. L.: Surficial geology, Carcajou Canyon, Northwest Territories, Map 1988A, Geological Survey of Canada, https://doi.org/10.4095/213616, 2002.

Duk-Rodkin, A. and Lemmen, S.: Glacial history of the Mackenzie region, The physical environment of the Mackenzie Valley, Northwest Territories: a base line for the assessment of environmental change, Geological Survey of Canada Bulletin, ISBN 0-660-19564-X, 2000.

Dulfer, H. E., Stoker, B. J., Margold, M., and Stokes, C. R.: Glacial geomorphology of the northwest Laurentide Ice Sheet on the northern Interior Plains and western Canadian Shield, Canada, J. Maps, 19, 2181714, https://doi.org/10.1080/17445647.2023.2181714, 2023.

Dyke, A. S. and Evans, D. J. A.: Ice-marginal terrestrial landsystems: Northern Laurentide and Innuitian ice sheet margins, in: Glacial Landsystems, Routledge, ISBN 9780340806661, 2005.

Dyke, A. S. and Prest, V. K.: Late Wisconsinan and Holocene retreat of the Laurentide Ice Sheet, Geological Survey of Canada, https://doi.org/10.7202/032681ar, 1987.

Ewing, S. A., O'Donnell, J. A., Aiken, G. R., Butler, K., Butman, D., Windham-Myers, L., and Kanevskiy, M. Z.: Long-term anoxia and release of ancient, labile carbon upon thaw of Pleistocene permafrost, Geophys. Res. Lett., 42, https://doi.org/10.1002/2015GL066296, 2015.

Fouché, J., Christiansen, C. T., Lafrenière, M. J., Grogan, P., and Lamoureux, S. F.: Canadian permafrost stores large pools of ammonium and optically distinct dissolved organic matter, Nat. Commun., 11, 4500, https://doi.org/10.1038/s41467-020-18331-w, 2020.

Fraser, T. A. and Burn, C. R.: On the nature and origin of "muck" deposits in the Klondike area, Yukon Territory, Can. J. Earth Sci., 34, 1333–1344, https://doi.org/10.1139/e17-106, 1997.

Froese, D., Westgate, J., Preece, S., and Storer, J.: Age and significance of the Late Pleistocene Dawson tephra in eastern Beringia, Quat. Sci. Rev., 21, 2137–2142, https://doi.org/10.1016/S0277-3791(02)00038-0, 2002.

Froese, D. G., Zazula, G. D., Westgate, J. A., Preece, S. J., Sanborn, P. T., Reyes, A. V., and Pearce, N. J. G.: The Klondike goldfields and Pleistocene environments of Beringia, GSA Today, 19, 4, https://doi.org/10.1130/GSATG54A.1, 2009.

Groeneveld, M., Catalán, N., Attermeyer, K., Hawkes, J., Einarsdóttir, K., Kothawala, D., Bergquist, J., and Tranvik, L.: Selective adsorption of terrestrial dissolved organic matter to inorganic surfaces along a boreal inland water continuum, J. Geophys. Res.-Biogeosci., 125, https://doi.org/10.1029/2019JG005236, 2020.

Groeneveld, M., Kothawala, D. N., and Tranvik, L. J.: Seasonally variable interactions between dissolved organic matter and mineral particles in an agricultural river, Aquat. Sci., 85, 2, https://doi.org/10.1007/s00027-022-00898-9, 2023.

Grosse, G., Romanovsky, V., Jorgenson, T., Anthony, K. W., Brown, J., and Overduin, P. P.: Vulnerability and feedbacks of permafrost to climate change, Eos, Transactions American Geophysical Union, 92, 73–74, https://doi.org/10.1029/2011EO090001, 2011.

Gu, B., Schmitt, J., Chen, Z., Liang, L., and McCarthy, J. F.: Adsorption and desorption of natural organic matter on iron oxide: mechanisms and models, Environ. Sci. Technol., 28, 38–46, https://doi.org/10.1021/es00050a007, 1994.

Guppy, C. N., Menzies, N. W., Moody, P. W., and Blamey, F. P. C.: Competitive sorption reactions between phosphorus and organic matter in soil: a review, Soil Res., 43, 189, https://doi.org/10.1071/SR04049, 2005.

Hanson, P. C., Bade, D. L., Carpenter, S. R., and Kratz, T. K.: Lake metabolism: Relationships with dissolved organic carbon and phosphorus, Limnol. Oceanogr., 48, 1112–1119, https://doi.org/10.4319/lo.2003.48.3.1112, 2003.

Harris, D., Horwáth, W. R., and Van Kessel, C.: Acid fumigation of soils to remove carbonates prior to total organic carbon or

carbon-13 isotopic analysis, Soil Sci. Soc. Am. J., 65, 1853–1856, https://doi.org/10.2136/sssaj2001.1853, 2001.

Hassink, J.: The capacity of soils to preserve organic C and N by their association with clay and silt particles, Plant Soil, 191, https://doi.org/10.1023/A:1004213929699, 1997.

Hatten, G. K. F., Kokelj, S. V., Opfergelt, S., Froese, D. G., Alvarez, A., Young, J. M., and Tank, S. E.: Biogeochemical characteristics and organic carbon sorption properties of permafrost-origin sediments from northwestern Canada, V1, Borealis [data set], https://doi.org/10.5683/SP3/NFOPAF, 2026.

Heginbottom, J. A., Dubreuil, M.-A., and Harker, P. T.: Canada, permafrost, MCR Series, Natural Resources Canada, Geomatics Canada, https://doi.org/10.4095/294672, 1995.

Helms, J. R., Stubbins, A., Ritchie, J. D., Minor, E. C., Kieber, D. J., and Mopper, K.: Absorption spectral slopes and slope ratios as indicators of molecular weight, source, and photobleaching of chromophoric dissolved organic matter, Limnol. Oceanogr., 53, 955–969, https://doi.org/10.4319/lo.2008.53.3.0955, 2008.

Herndon, E., AlBashaireh, A., Singer, D., Roy Chowdhury, T., Gu, B., and Graham, D.: Influence of iron redox cycling on organo-mineral associations in Arctic tundra soil, Geochim. Cosmochim. Ac., 207, 210–231, https://doi.org/10.1016/j.gca.2017.02.034, 2017.

Hernes, P. J., Robinson, A. C., and Aufdenkampe, A. K.: Fractionation of lignin during leaching and sorption and implications for organic matter "freshness", Geophys. Res. Lett., 34, 2007GL031017, https://doi.org/10.1029/2007GL031017, 2007.

Hilton, R. G., Galy, V., Gaillardet, J., Dellinger, M., Bryant, C., O'Regan, M., Gröcke, D. R., Coxall, H., Bouchez, J., and Calmels, D.: Erosion of organic carbon in the Arctic as a geological carbon dioxide sink, Nature, 524, 84–87, https://doi.org/10.1038/nature14653, 2015.

Hirst, C., Mauclet, E., Monhonval, A., Tihon, E., Ledman, J., Schuur, E. A. G., and Opfergelt, S.: Seasonal changes in hydrology and permafrost degradation control mineral element-bound DOC transport from permafrost soils to streams, Global Biogeochem. Cy., 36, e2021GB007105, https://doi.org/10.1029/2021GB007105, 2022.

Hubbard, C. R. and Snyder, R. L.: RIR – Measurement and Use in Quantitative XRD, Powder Diffr., 3, 74–77, https://doi.org/10.1017/S0885715600013257, 1988.

Jastrow, J. D., Boutton, T. W., and Miller, R. M.: Carbon dynamics of aggregate-associated organic matter estimated by Carbon-13 natural abundance, Soil Sci. Soc. Am. J., 60, 801–807, 1996.

Jongejans, L. L., Liebner, S., Knoblauch, C., Mangelsdorf, K., Ulrich, M., Grosse, G., Tanski, G., Fedorov, A. N., Konstantinov, P. Y., Windirsch, T., Wiedmann, J., and Strauss, J.: Greenhouse gas production and lipid biomarker distribution in Yedoma and Alas thermokarst lake sediments in Eastern Siberia, Glob. Change Biol., 27, 2822–2839, https://doi.org/10.1111/gcb.15566, 2021.

Jorgenson, M. T., Kanevskiy, M., Shur, Y., Moskalenko, N., Brown, D. R. N., Wickland, K., Striegl, R., and Koch, J.: Role of ground ice dynamics and ecological feedbacks in recent ice wedge degradation and stabilization, J. Geophys. Res.-Earth, 120, 2280–2297, https://doi.org/10.1002/2015JF003602, 2015.

Kaiser, K. and Guggenberger, G.: The role of DOM sorption to mineral surfaces in the preservation of organic matter in soils, Org. Geochem., 31, 711–725, https://doi.org/10.1016/S0146-6380(00)00046-2, 2000.

Kaiser, K. and Zech, W.: Competitive sorption of dissolved organic matter fractions to soils and related mineral phases, Soil Sci. Soc. Am. J., 61, 64–69, https://doi.org/10.2136/sssaj1997.03615995006100010011x, 1997.

Kaiser, K., Guggenberger, G., and Zech, W.: Sorption of DOM and DOM fractions to forest soils, Geoderma, 74, 281–303, https://doi.org/10.1016/S0016-7061(96)00071-7, 1996.

Kaiser, K., Kaupenjohann, M., and Zech, W.: Sorption of dissolved organic carbon in soils: effects of soil sample storage, soil-to-solution ratio, and temperature, Geoderma, 99, 317–328, https://doi.org/10.1016/S0016-7061(00)00077-X, 2001.

Kalbitz, K., Schmerwitz, J., Schwesig, D., and Matzner, E.: Biodegradation of soil-derived dissolved organic matter as related to its properties, Geoderma, 113, 273–291, https://doi.org/10.1016/S0016-7061(02)00365-8, 2003.

Kalbitz, K., Schwesig, D., Rethemeyer, J., and Matzner, E.: Stabilization of dissolved organic matter by sorption to the mineral soil, Soil Biol. Biochem., 37, 1319–1331, https://doi.org/10.1016/j.soilbio.2004.11.028, 2005.

Kawahigashi, M., Kaiser, K., Rodionov, A., and Guggenberger, G.: Sorption of dissolved organic matter by mineral soils of the Siberian forest tundra: DOM sorption on permafrost-affected soils, Glob. Change Biol., 12, 1868–1877, https://doi.org/10.1111/j.1365-2486.2006.01203.x, 2006.

Keller, K., Blum, J. D., and Kling, G. W.: Stream geochemistry as an indicator of increasing permafrost thaw depth in an arctic watershed, Chem. Geol., 273, 76–81, https://doi.org/10.1016/j.chemgeo.2010.02.013, 2010.

Kennedy, K. E., Froese, D. G., Zazula, G. D., and Lauriol, B.: Last Glacial Maximum age for the northwest Laurentide maximum from the Eagle River spillway and delta complex, northern Yukon, Quat. Sci. Rev., 29, 1288–1300, https://doi.org/10.1016/j.quascirev.2010.02.015, 2010.

Keskitalo, K. H., Bröder, L., Shakil, S., Zolkos, S., Tank, S. E., van Dongen, B. E., Tesi, T., Haghipour, N., Eglinton, T. I., Kokelj, S. V., and Vonk, J. E.: Downstream evolution of particulate organic matter composition from permafrost thaw slumps, Front. Earth Sci., 9, 642675, https://doi.org/10.3389/feart.2021.642675, 2021.

Kleber, M., Nico, P. S., Plante, A., Filley, T., Kramer, M., Swanston, C., and Sollins, P.: Old and stable soil organic matter is not necessarily chemically recalcitrant: implications for modeling concepts and temperature sensitivity, Glob. Change Biol., 17, 1097–1107, https://doi.org/10.1111/j.1365-2486.2010.02278.x, 2011.

Kokelj, S. V., Jenkins, R. E., Milburn, D., Burn, C. R., and Snow, N.: The influence of thermokarst disturbance on the water quality of small upland lakes, Mackenzie Delta region, Northwest Territories, Canada, Permafrost Periglac., 16, 343–353, https://doi.org/10.1002/ppp.536, 2005.

Kokelj, S. V., Lacelle, D., Lantz, T. C., Tunnicliffe, J., Malone, L., Clark, I. D., and Chin, K. S.: Thawing of massive ground ice in mega slumps drives increases in stream sediment and solute flux across a range of watershed scales, J. Geophys. Res.-Earth, 118, 681–692, https://doi.org/10.1002/jgrf.20063, 2013.

Kokelj, S. V., Tunnicliffe, J., Lacelle, D., Lantz, T. C., Chin, K. S., and Fraser, R.: Increased precipitation drives mega slump development and destabilization of ice-rich permafrost ter-

rain, northwestern Canada, Global Planet. Change, 129, 56–68, https://doi.org/10.1016/j.gloplacha.2015.02.008, 2015.

Kokelj, S. V., Lantz, T. C., Tunnicliffe, J., Segal, R., and Lacelle, D.: Climate-driven thaw of permafrost preserved glacial landscapes, northwestern Canada, Geology, 45, 371–374, https://doi.org/10.1130/G38626.1, 2017a.

Kokelj, S. V., Tunnicliffe, J., and Lacelle, D.: The Peel plateau of Northwestern Canada: An ice-rich hummocky moraine landscape in transition, in: Landscapes and Landforms of Western Canada, edited by: Slaymaker, O., Springer International Publishing, Switzerland, 109–122, ISBN 3319445936, 2017b.

Kokelj, S. V., Kokoszka, J., van der Sluijs, J., Rudy, A. C. A., Tunnicliffe, J., Shakil, S., Tank, S. E., and Zolkos, S.: Thaw-driven mass wasting couples slopes with downstream systems, and effects propagate through Arctic drainage networks, The Cryosphere, 15, 3059–3081, https://doi.org/10.5194/tc-15-3059-2021, 2021.

Kokelj, S. V., Gingras-Hill, T., Daly, S. V., Morse, P., Wolfe, S., Rudy, A. C. A., Van Der Sluijs, J., Weiss, N., O'Neill, B., Baltzer, J., Lantz, T. C., Gibson, C., Cazon, D., Fraser, R. H., Froese, D. G., Giff, G., Klengenberg, C., Lamoureux, S. F., Quinton, W., Turetsky, M. R., Chiasson, A., Ferguson, C., Newton, M., Pope, M., Paul, J. A., Wilson, A., and Young, J.: The Northwest Territories Thermokarst Mapping Collective: A northern-driven mapping collaborative toward understanding the effects of permafrost thaw, Arctic Science, 9, 886–918, https://doi.org/10.1139/AS-2023-0009, 2023.

Kokelj, S. V., Wolfe, S. A., Weiss, N., Froese, D., Baltzer, J. L., Lantz, T., O'Neill, B., Morse, P. D., Sniderhan, A., Speetjens, N. J., Van Der Sluijs, J., Alvarez, A., Tank, S. E., and Gruber, S.: Permafrost landsystems define regional variability in climate change effects on northern environments, Nat. Commun., https://doi.org/10.1038/s41467-026-71216-2, 2026.

Kothawala, D. N., Moore, T. R., and Hendershot, W. H.: Adsorption of dissolved organic carbon to mineral soils: A comparison of four isotherm approaches, Geoderma, 148, 43–50, https://doi.org/10.1016/j.geoderma.2008.09.004, 2008.

Kothawala, D. N., Moore, T. R., and Hendershot, W. H.: Soil properties controlling the adsorption of dissolved organic carbon to mineral soils, Soil Sci. Soc. Am. J., 73, 1831–1842, https://doi.org/10.2136/sssaj2008.0254, 2009.

Kothawala, D. N., Stedmon, C. A., Müller, R. A., Weyhenmeyer, G. A., Köhler, S. J., and Tranvik, L. J.: Controls of dissolved organic matter quality: evidence from a large-scale boreal lake survey, Glob. Change Biol., 20, 1101–1114, https://doi.org/10.1111/gcb.12488, 2014.

Kuhry, P., Bárta, J., Blok, D., Elberling, B., Faucherre, S., Hugelius, G., Jørgensen, C. J., Richter, A., Šantrůčková, H., and Weiss, N.: Lability classification of soil organic matter in the northern permafrost region, Biogeosciences, 17, 361–379, https://doi.org/10.5194/bg-17-361-2020, 2020.

Lacelle, D., Bjornson, J., Lauriol, B., Clark, I., and Troutet, Y.: Segregated-intrusive ice of subglacial meltwater origin in retrogressive thaw flow headwalls, Richardson Mountains, NWT, Canada, Quat. Sci. Rev., 23, 681–696, https://doi.org/10.1016/j.quascirev.2003.09.005, 2004.

Lacelle, D., Bjornson, J., and Lauriol, B.: Climatic and geomorphic factors affecting contemporary (1950–2004) activity of retrogressive thaw slumps on the Aklavik Plateau, Richardson Mountains, NWT, Canada, Permafrost Periglac., 21, 1–15, https://doi.org/10.1002/ppp.666, 2010.

Lacelle, D., Lauriol, B., Zazula, G., Ghaleb, B., Utting, N., and Clark, I. D.: Timing of advance and basal condition of the Laurentide Ice Sheet during the last glacial maximum in the Richardson Mountains, NWT, Quaternary Res., 80, 274–283, https://doi.org/10.1016/j.yqres.2013.06.001, 2013.

Lacelle, D., Fontaine, M., Pellerin, A., Kokelj, S. V., and Clark, I. D.: Legacy of Holocene landscape changes on soil biogeochemistry: A perspective from paleo-active layers in Northwestern Canada, J. Geophys. Res.-Biogeosci., 124, 2662–2679, https://doi.org/10.1029/2018JG004916, 2019.

Lau, M. P., Hutchins, R. H. S., Tank, S. E., and A. Del Giorgio, P.: The chemical succession in anoxic lake waters as source of molecular diversity of organic matter, Sci. Rep.-UK, 14, 3831, https://doi.org/10.1038/s41598-024-54387-0, 2024.

Lipovsky, P. S., Coates, J., Lewkowicz, A. G., and Trochim, E.: Active-layer detachments following the summer 2004 forest fires near Dawson City, Yukon, Yukon Exploration and Geology 2005, Yukon Geological Survey, https://www.emrlibrary.gov.yk.ca/emrlibrary/ygs/yeg/2005/2005_p175-194.pdf (last access: 10 November 2024), 2005.

Littlefair, C. A. and Tank, S. E.: Biodegradability of thermokarst carbon in a till-associated, glacial margin landscape: The case of the Peel Plateau, NWT, Canada, J. Geophys. Res.-Biogeosci., 123, 3293–3307, https://doi.org/10.1029/2018JG004461, 2018.

Littlefair, C. A., Tank, S. E., and Kokelj, S. V.: Retrogressive thaw slumps temper dissolved organic carbon delivery to streams of the Peel Plateau, NWT, Canada, Biogeosciences, 14, 5487–5505, https://doi.org/10.5194/bg-14-5487-2017, 2017.

Lu, Y., Wassmann, R., Neue, H.-U., and Huang, C.: Dynamics of dissolved organic carbon and methane emissions in a flooded rice soil, Soil Sci. Soc. Am. J., 64, 2011–2017, https://doi.org/10.2136/sssaj2000.6462011x, 2000.

MacDonald, E. N., Tank, S. E., Kokelj, S. V., Froese, D. G., and Hutchins, R. H. S.: Permafrost-derived dissolved organic matter composition varies across permafrost end-members in the western Canadian Arctic, Environ. Res. Lett., 16, 024036, https://doi.org/10.1088/1748-9326/abd971, 2021.

MacDonald, E. N., Saidi-Mehrabad, A., Lanoil, B., Lech, G., and Tank, S.: Coupled shifts in DOM composition and microbial community structure lead to variable biodegradation rates in thermokarst-affected permafrost stratigraphies, Arctic Science, 11, 1–17, https://doi.org/10.1139/as-2024-0050, 2025.

Mackay, J. R.: The world of underground ice, Ann. Assoc. Am. Geogr., 62, 1–22, https://doi.org/10.1111/j.1467-8306.1972.tb00839.x, 1972.

Mahony, M. E.: 50 000 years of paleoenvironmental change recorded in meteoric waters and coeval paleoecological and cryostratigraphic indicators from the Klondike goldfields, Yukon, Canada, University of Alberta, https://doi.org/10.7939/R34T6FF58, 2015.

Malone, L., Lacelle, D., Kokelj, S., and Clark, I. D.: Impacts of hillslope thaw slumps on the geochemistry of permafrost catchments (Stony Creek watershed, NWT, Canada), Chem. Geol., 356, 38–49, https://doi.org/10.1016/j.chemgeo.2013.07.010, 2013.

Mann, P. J., Eglinton, T. I., McIntyre, C. P., Zimov, N., Davydova, A., Vonk, J. E., Holmes, R. M., and Spencer, R. G. M.: Utilization of ancient permafrost carbon in head-

waters of Arctic fluvial networks, Nat. Commun., 6, 7856, https://doi.org/10.1038/ncomms8856, 2015.

Martens, J., Mueller, C. W., Joshi, P., Rosinger, C., Maisch, M., Kappler, A., Bonkowski, M., Schwamborn, G., Schirrmeister, L., and Rethemeyer, J.: Stabilization of mineral-associated organic carbon in Pleistocene permafrost, Nat. Commun., 14, 2120, https://doi.org/10.1038/s41467-023-37766-5, 2023.

Monhonval, A., Strauss, J., Mauclet, E., Hirst, C., Bemelmans, N., Grosse, G., Schirrmeister, L., Fuchs, M., and Opfergelt, S.: Iron redistribution upon thermokarst processes in the Yedoma domain, Front. Earth Sci., 9, 703339, https://doi.org/10.3389/feart.2021.703339, 2021a.

Monhonval, A., Mauclet, E., Pereira, B., Vandeuren, A., Strauss, J., Grosse, G., Schirrmeister, L., Fuchs, M., Kuhry, P., and Opfergelt, S.: Mineral element stocks in the Yedoma domain: A novel method applied to ice-rich permafrost regions, Front. Earth Sci., 9, 703304, https://doi.org/10.3389/feart.2021.703304, 2021b.

Monhonval, A., Strauss, J., Thomas, M., Hirst, C., Titeux, H., Louis, J., Gilliot, A., du Bois d'Aische, E., Pereira, B., Vandeuren, A., Grosse, G., Schirrmeister, L., Jongejans, L. L., Ulrich, M., and Opfergelt, S.: Thermokarst processes increase the supply of stabilizing surfaces and elements (Fe, Mn, Al, and Ca) for mineral–organic carbon interactions, Permafrost Periglac., 33, 452–469, https://doi.org/10.1002/ppp.2162, 2022.

Monteath, A. J., Kuzmina, S., Mahony, M., Calmels, F., Porter, T., Mathewes, R., Sanborn, P., Zazula, G., Shapiro, B., Murchie, T. J., Poinar, H. N., Sadoway, T., Hall, E., Hewitson, S., and Froese, D.: Relict permafrost preserves megafauna, insects, pollen, soils and pore-ice isotopes of the mammoth steppe and its collapse in central Yukon, Quat. Sci. Rev., 299, 107878, https://doi.org/10.1016/j.quascirev.2022.107878, 2023.

Mortensen, J. K.: Geology and U–Pb geochronology of the Klondike District, west-central Yukon Territory, Can. J. Earth Sci., 27, 903–914, https://doi.org/10.1139/e90-093, 1990.

Mu, C. C., Abbott, B. W., Wu, X. D., Zhao, Q., Wang, H. J., Su, H., Wang, S. F., Gao, T. G., Guo, H., Peng, X. Q., and Zhang, T. J.: Thaw depth determines dissolved organic carbon concentration and biodegradability on the Northern Qinghai-Tibetan Plateau, Geophys. Res. Lett., 44, 9389–9399, https://doi.org/10.1002/2017GL075067, 2017.

Murchie, T. J., Monteath, A. J., Mahony, M. E., Long, G. S., Cocker, S., Sadoway, T., Karpinski, E., Zazula, G., MacPhee, R. D. E., Froese, D., and Poinar, H. N.: Collapse of the mammoth-steppe in central Yukon as revealed by ancient environmental DNA, Nat. Commun., 12, 7120, https://doi.org/10.1038/s41467-021-27439-6, 2021.

Murphy, K. R., Stedmon, C. A., Graeber, D., and Bro, R.: Fluorescence spectroscopy and multi-way techniques. PARAFAC, Anal. Methods, 5, 6557, https://doi.org/10.1039/c3ay41160e, 2013.

Nodvin, S., Driscoll, C., and Likens, G.: Simple partitioning of anions and dissolved organic carbon in a forest soil, Soil Sci., 27–35, 1986.

Norris, D. K.: Geology, northern Yukon Territory and northwestern District of Mackenzie, Open File, Geological Survey of Canada, https://doi.org/10.4095/129102, 1980.

Oksanen, J., Simpson, G. L., Blanchet, F. G., Kindt, R., Legendre, P., Minchin, P. R., O'Hara, R. B., Solymos, P., Stevens, M. H. H., Szoecs, E., Wagner, H., Barbour, M., Bedward, M., Bolker, B., Borcard, D., Carvalho, G., Chirico, M., Caceres, M. D., Durand, S., Evangelista, H. B. A., FitzJohn, R., Friendly, M., Furneaux, B., Hannigan, G., Hill, M. O., Lahti, L., McGlinn, D., Ouellette, M.-H., Cunha, E. R., Smith, T., Stier, A., Braak, C. J. F. T., and Weedon, J.: vegan: Community ecology package (2.6-8), CRAN R-Package, https://cran.r-project.org/web/packages/vegan/index.html (last access: 12 November 2024), 2024.

Okulitch, A. V. and Irwin, D.: Geological compilation of the western mainland and Arctic islands of the Northwest Territories, Northwest Territories Geological Survey, https://ntgs-open-data-ntgs.hub.arcgis.com/datasets/369a2fe1a6604ce7b270965fbea1a7e0/about (last access: 8 November 2024), 2017.

O'Neill, H. B., Wolfe, S. A., and Duchesne, C.: New ground ice maps for Canada using a paleogeographic modelling approach, The Cryosphere, 13, 753–773, https://doi.org/10.5194/tc-13-753-2019, 2019.

O'Neill, H. B., Smith, S. L., Burn, C. R., Duchesne, C., and Zhang, Y.: Widespread permafrost degradation and thaw subsidence in northwest Canada, J. Geophys. Res.-Earth, 128, e2023JF007262, https://doi.org/10.1029/2023JF007262, 2023.

Opfergelt, S.: The next generation of climate model should account for the evolution of mineral-organic interactions with permafrost thaw, Environ. Res. Lett., 15, 091003, https://doi.org/10.1088/1748-9326/ab9a6d, 2020.

Opfergelt, S., Herndon, E. M., Bryce, C., Barker, A. J., and Hirst, C.: Iron as a driver of organic carbon fate in permafrost regions, Nat. Geosci., 19, 750–758, https://doi.org/10.1038/s41561-026-02015-z, 2026.

Pansu, M. and Gautheyrou, J.: Handbook of Soil Analysis Mineralogical, Organic and Inorganic Methods, Springer, Berlin, ISBN 3540312102, 2006.

Parfitt, R. and Childs, C.: Estimation of forms of Fe and Al – a review, and analysis of contrasting soils by dissolution and Mossbauer methods, Soil Res., 26, 121, https://doi.org/10.1071/SR9880121, 1988.

Peter, S., Isidorova, A., and Sobek, S.: Enhanced carbon loss from anoxic lake sediment through diffusion of dissolved organic carbon: DOC flux from anoxic lake sediments, J. Geophys. Res.-Biogeosci., 121, 1959–1977, https://doi.org/10.1002/2016JG003425, 2016.

Péwé, T. L.: Quarternary geology of Alaska, Geological Survery Professional Paper 835, United States, https://dggs.alaska.gov/webpubs/usgs/p/text/p0835.pdf (last access: 3 February 2025), 1975.

Ramnarine, R., Voroney, R. P., Wagner-Riddle, C., and Dunfield, K. E.: Carbonate removal by acid fumigation for measuring the δ^{13}C of soil organic carbon, Can. J. Soil. Sci., 91, 247–250, https://doi.org/10.4141/cjss10066, 2011.

Rasmussen, C., Torn, M. S., and Southard, R. J.: Mineral assemblage and aggregates control carbon dynamics in a California conifer forest, Soil Sci. Soc. Am. J., 69, 1711–1721, https://doi.org/10.2136/sssaj2005.0040, 2005.

Rasmussen, C., Heckman, K., Wieder, W. R., Keiluweit, M., Lawrence, C. R., Berhe, A. A., Blankinship, J. C., Crow, S. E., Druhan, J. L., Hicks Pries, C. E., Marin-Spiotta, E., Plante, A. F., Schädel, C., Schimel, J. P., Sierra, C. A., Thompson, A., and Wagai, R.: Beyond clay: Towards an improved set of variables for predicting soil organic matter content, Biogeochemistry, 137, 297–306, https://doi.org/10.1007/s10533-018-0424-3, 2018.

R Core Team: R: A language environment for statistical computing, https://www.R-project.org/ (last access: 12 November 2024), 2024.

Saidy, A. R., Smernik, R. J., Baldock, J. A., Kaiser, K., and Sanderman, J.: The sorption of organic carbon onto differing clay minerals in the presence and absence of hydrous iron oxide, Geoderma, 209–210, 15–21, https://doi.org/10.1016/j.geoderma.2013.05.026, 2013.

Sanborn, P. T., Smith, C. A. S., Froese, D. G., Zazula, G. D., and Westgate, J. A.: Full-glacial paleosols in perennially frozen loess sequences, Klondike goldfields, Yukon Territory, Canada, Quaternary Res., 66, 147–157, https://doi.org/10.1016/j.yqres.2006.02.008, 2006.

Schirrmeister, L., Kunitsky, V., Grosse, G., Wetterich, S., Meyer, H., Schwamborn, G., Babiy, O., Derevyagin, A., and Siegert, C.: Sedimentary characteristics and origin of the Late Pleistocene Ice Complex on north-east Siberian Arctic coastal lowlands and islands – A review, Quatern. Int., 241, 3–25, https://doi.org/10.1016/j.quaint.2010.04.004, 2011.

Schirrmeister, L., Froese, D., Tumskoy, V., Grosse, G., and Wetterich, S.: Permafrost and periglacial features | Yedoma: Late Pleistocene ice-rich syngenetic permafrost of Beringia, in: Encyclopedia of Quaternary Science, Elsevier, 542–552, https://doi.org/10.1016/B978-0-444-53643-3.00106-0, 2013.

Schirrmeister, L., Froese, D., Wetterich, S., Strauss, J., Veremeeva, A., and Grosse, G.: Yedoma: Late Pleistocene ice-rich syngenetic permafrost of Beringia, in: Encyclopedia of Quaternary Science, Elsevier, 296–311, https://doi.org/10.1016/B978-0-323-99931-1.00223-3, 2024.

Shakil, S., Tank, S. E., Kokelj, S. V., Vonk, J. E., and Zolkos, S.: Particulate dominance of organic carbon mobilization from thaw slumps on the Peel Plateau, NT: Quantification and implications for stream systems and permafrost carbon release, Environ. Res. Lett., 15, 114019, https://doi.org/10.1088/1748-9326/abac36, 2020.

Shakil, S., Tank, S. E., Vonk, J. E., and Zolkos, S.: Low biodegradability of particulate organic carbon mobilized from thaw slumps on the Peel Plateau, NT, and possible chemosynthesis and sorption effects, Biogeosciences, 19, 1871–1890, https://doi.org/10.5194/bg-19-1871-2022, 2022.

Speetjens, N. J., Tanski, G., Martin, V., Wagner, J., Richter, A., Hugelius, G., Boucher, C., Lodi, R., Knoblauch, C., Koch, B. P., Wünsch, U., Lantuit, H., and Vonk, J. E.: Dissolved organic matter characterization in soils and streams in a small coastal low-Arctic catchment, Biogeosciences, 19, 3073–3097, https://doi.org/10.5194/bg-19-3073-2022, 2022.

Spencer, R. G. M., Mann, P. J., Dittmar, T., Eglinton, T. I., McIntyre, C., Holmes, R. M., Zimov, N., and Stubbins, A.: Detecting the signature of permafrost thaw in Arctic rivers, Geophys. Res. Lett., 42, 2830–2835, https://doi.org/10.1002/2015GL063498, 2015.

Statistics Canada: Provinces/Territories, Digital Boundary File – 2016 Census, https://open.canada.ca/data/en/dataset/47bd4f2e-1c77-49f8-8406-dc4dca64ee6b (last access: 18 February 2025), 2016.

Strauss, J., Schirrmeister, L., Wetterich, S., Borchers, A., and Davydov, S. P.: Grain-size properties and organic-carbon stock of Yedoma Ice Complex permafrost from the Kolyma lowland, northeastern Siberia, Global Biogeochem. Cy., 26, 2011GB004104, https://doi.org/10.1029/2011GB004104, 2012.

Strauss, J., Schirrmeister, L., Grosse, G., Wetterich, S., Ulrich, M., Herzschuh, U., and Hubberten, H.: The deep permafrost carbon pool of the Yedoma region in Siberia and Alaska, Geophys. Res. Lett., 40, 6165–6170, https://doi.org/10.1002/2013GL058088, 2013.

Szymański, W., Drewnik, M., Stolarczyk, M., Musielok, Ł., Gus-Stolarczyk, M., and Skiba, M.: Occurrence and stability of organic intercalation in clay minerals from permafrost-affected soils in the High Arctic – A case study from Spitsbergen (Svalbard), Geoderma, 408, 115591, https://doi.org/10.1016/j.geoderma.2021.115591, 2022.

Tank, S. E., Vonk, J. E., Walvoord, M. A., McClelland, J. W., Laurion, I., and Abbott, B. W.: Landscape matters: Predicting the biogeochemical effects of permafrost thaw on aquatic networks with a state factor approach, Permafrost Periglac., 31, 358–370, https://doi.org/10.1002/ppp.2057, 2020.

The MathWorks Inc.: MATLAB version: 23.2.0 (R2023b), https://www.mathworks.com (last access: 12 November 2024), 2023.

Thomas, M., Monhonval, A., Hirst, C., Bröder, L., Zolkos, S., Vonk, J. E., Tank, S. E., Keskitalo, K. H., Shakil, S., Kokelj, S. V., Van Der Sluijs, J., and Opfergelt, S.: Evidence for preservation of organic carbon interacting with iron in material displaced from retrogressive thaw slumps: Case study in Peel Plateau, western Canadian Arctic, Geoderma, 433, 116443, https://doi.org/10.1016/j.geoderma.2023.116443, 2023.

Torn, M. S., Trumbore, S. E., Chadwick, O. A., Vitousek, P. M., and Hendricks, D. M.: Mineral control of soil organic carbon storage and turnover, Nature, 389, 170–173, https://doi.org/10.1038/38260, 1997.

Vance, G. F. and David, M. B.: Effect of acid treatment on dissolved organic carbon retention by a spodic horizon, Soil Sci. Soc. Am. J., 53, 1242–1247, https://doi.org/10.2136/sssaj1989.03615995005300040042x, 1989.

Voggenreiter, E., Scmitt-Kopplin, P., ThomasArrigo, L., Bryce, C., Kappler, A., and Joshi, P.: Emerging investigator series: preferential adsorption and coprecipitation of permafrost organic matter with poorly crystalline iron minerals, Environ. Sci.-Proc. Imp., https://doi.org/10.1039/D4EM00241E, 2024.

Vonk, J. E., Mann, P. J., Davydov, S., Davydova, A., Spencer, R. G. M., Schade, J., Sobczak, W. V., Zimov, N., Zimov, S., Bulygina, E., Eglinton, T. I., and Holmes, R. M.: High biolability of ancient permafrost carbon upon thaw, Geophys. Res. Lett., 40, 2689–2693, https://doi.org/10.1002/grl.50348, 2013.

Vonk, J. E., Tank, S. E., and Walvoord, M. A.: Integrating hydrology and biogeochemistry across frozen landscapes, Nat. Commun., 10, 5377, https://doi.org/10.1038/s41467-019-13361-5, 2019.

Vonk, J. E., Fritz, M., Speetjens, N. J., Babin, M., Bartsch, A., Basso, L. S., Bröder, L., Göckede, M., Gustafsson, Ö., Hugelius, G., Irrgang, A. M., Juhls, B., Kuhn, M. A., Lantuit, H., Manizza, M., Martens, J., O'Regan, M., Suslova, A., Tank, S. E., Terhaar, J., and Zolkos, S.: The land–ocean Arctic carbon cycle, Nat. Rev. Earth Environ., 6, 86–105, https://doi.org/10.1038/s43017-024-00627-w, 2025.

von Lützow, M., Kögel-Knabner, I., Ekschmitt, K., Matzner, E., Guggenberger, G., Marschner, B., and Flessa, H.: Stabilization of organic matter in temperate soils: Mechanisms and their rele-

vance under different soil conditions – a review, Eur. J. Soil. Sci., 57, 426–445, https://doi.org/10.1111/j.1365-2389.2006.00809.x, 2006.

Walvoord, M. A. and Kurylyk, B. L.: Hydrologic impacts of thawing permafrost – A Review, Vadose Zone J., 15, 1–20, https://doi.org/10.2136/vzj2016.01.0010, 2016.

Wang, Y., Guo, Y., Wang, X., Song, C., Song, Y., Liu, Z., Wang, S., Gao, S., and Ma, G.: Mineral protection controls soil organic carbon stability in permafrost wetlands, Sci. Total Environ., 869, 161864, https://doi.org/10.1016/j.scitotenv.2023.161864, 2023.

Weishaar, J. L., Aiken, G. R., Bergamaschi, B. A., Fram, M. S., Fujii, R., and Mopper, K.: Evaluation of specific ultraviolet absorbance as an indicator of the chemical composition and reactivity of dissolved organic carbon, Environ. Sci. Technol., 37, 4702–4708, https://doi.org/10.1021/es030360x, 2003.

Wickham, H.: ggplot2: Elegant graphics for data analysis, Springer-Verlag New York, ISBN 978-3-319-24277-4, 2016.

Wickham, H., François, R., Henry, L., Müller, K., and Vaughan, D.: dplyr: A grammar of data manipulation, CRAN, https://doi.org/10.32614/CRAN.package.dplyr, 2023.

Wickland, K. P., Waldrop, M. P., Aiken, G. R., Koch, J. C., Jorgenson, M. T., and Striegl, R. G.: Dissolved organic carbon and nitrogen release from boreal Holocene permafrost and seasonally frozen soils of Alaska, Environ. Res. Lett., 13, 065011, https://doi.org/10.1088/1748-9326/aac4ad, 2018.

Wolfe, S., Murton, J., Bateman, M., and Barlow, J.: Oriented-lake development in the context of late Quaternary landscape evolution, McKinley Bay Coastal Plain, western Arctic Canada, Quat. Sci. Rev., 242, 106414, https://doi.org/10.1016/j.quascirev.2020.106414, 2020.

Yavitt, J. B.: Methane and carbon dioxide dynamics in Typha Latifolia (L.) wetlands in central New York state, Wetlands, 17, 13, https://doi.org/10.1007/BF03161429, 1997.

Young, J. M., Alvarez, A., Van Der Sluijs, J., Kokelj, S. V., Rudy, A., McPhee, A., Stoker, B. J., Margold, M., and Froese, D.: Recent intensification (2004–2020) of permafrost mass-wasting in the central Mackenzie Valley foothills is a legacy of past forest fire disturbances, Geophys. Res. Lett., 49, https://doi.org/10.1029/2022GL100559, 2022.

Young, J. M., van der Sluijs, J., Kokelj, S. V., Gruber, S., Herring, T., Rudy, A. C. A., Alvarez, A., and Froese, D.: Permafrost detachment slides: A distinct high-magnitude permafrost mass wasting process, Geophys. Res. Lett., 53, e2026GL124103, https://doi.org/10.1029/2026GL124103, 2026.

Zolkos, S. and Tank, S. E.: Permafrost geochemistry and retrogressive thaw slump morphology (Peel Plateau, Canada), v.1.0 (2017–2017), Nordicana D45 [data set], https://doi.org/10.5885/45573XD-28DD57D553F14BF0, 2019.

Zolkos, S. and Tank, S. E.: Experimental evidence that permafrost thaw history and mineral composition shape abiotic carbon cycling in thermokarst-affected stream networks, Front. Earth Sci., 8, 152, https://doi.org/10.3389/feart.2020.00152, 2020.

Zolkos, S., Tank, S. E., and Kokelj, S. V.: Mineral weathering and the permafrost carbon-climate feedback, Geophys. Res. Lett., 45, 9623–9632, https://doi.org/10.1029/2018GL078748, 2018.

Zolkos, S., Tank, S. E., Striegl, R. G., and Kokelj, S. V.: Thermokarst effects on carbon dioxide and methane fluxes in streams on the Peel Plateau (NWT, Canada), J. Geophys. Res.-Biogeosci., 124, 1781–1798, https://doi.org/10.1029/2019JG005038, 2019.

Zolkos, S., Tank, S. E., Striegl, R. G., Kokelj, S. V., Kokoszka, J., Estop-Aragonés, C., and Olefeldt, D.: Thermokarst amplifies fluvial inorganic carbon cycling and export across watershed scales on the Peel Plateau, Canada, Biogeosciences, 17, 5163–5182, https://doi.org/10.5194/bg-17-5163-2020, 2020.

Zolkos, S., Tank, S. E., Kokelj, S. V., Striegl, R. G., Shakil, S., Voigt, C., Sonnentag, O., Quinton, W. L., Schuur, E. A. G., Zona, D., Lafleur, P. M., Sullivan, R. C., Ueyama, M., Billesbach, D., Cook, D., Humphreys, E. R., and Marsh, P.: Permafrost landscape history shapes fluvial chemistry, ecosystem carbon balance, and potential trajectories of future change, Global Biogeochem. Cy., 36, https://doi.org/10.1029/2022GB007403, 2022.

Zoltai, S. C.: Cyclic development of permafrost in the peatlands of Northwestern Alberta, Canada, Arctic Alpine Res., 25, 240–246, https://doi.org/10.1080/00040851.1993.12003011, 1993.